IJC
International Journal of Cancer

Epithelial–mesenchymal transition in human gastric cancer cell lines induced by TNF-α-inducing protein of *Helicobacter pylori*

Tatsuro Watanabe[1], Atsushi Takahashi[1,2], Kaori Suzuki[1], Miki Kurusu-Kanno[1], Kensei Yamaguchi[3], Hirota Fujiki[1] and Masami Suganuma[1]

[1] Research Institute for Clinical Oncology, Saitama Cancer Center, Kitaadachi-gun, Saitama, Japan
[2] Graduate School of Science and Engineering, Saitama University, Sakura-ku, Saitama, Japan
[3] Saitama Cancer Center Hospital, Kitaadachi-gun, Saitama, Japan

Helicobacter pylori strains produce tumor necrosis factor-α (TNF-α)-inducing protein, Tipα as a carcinogenic factor in the gastric epithelium. Tipα acts as a homodimer with 38-kDa protein, whereas del-Tipα is an inactive monomer. *H. pylori* isolated from gastric cancer patients secreted large amounts of Tipα, which are incorporated into gastric cancer cells by directly binding to nucleolin on the cell surface, which is a receptor of Tipα. The binding complex induces expression of *TNF-α* and *chemokine* genes, and activates NF-κB (nuclear factor kappa-light-chain-enhancer of activated B cells). To understand the mechanisms of Tipα in tumor progression, we looked at numerous effects of Tipα on human gastric cancer cell lines. Induction of cell migration and elongation was found to be mediated through the binding to surface nucleolin, which was inhibited by the nucleolin-targeted siRNAs. Tipα induced formation of filopodia in MKN-1 cells, suggesting invasive morphological changes. Tipα enhanced the phosphorylation of 11 cancer-related proteins in serine, threonine and tyrosine, indicating activation of MEK-ERK signal cascade. Although the downregulation of E-cadherin was not shown in MKN-1 cells, Tipα induced the expression of vimentin, a significant marker of the epithelial–mesenchymal transition (EMT). It is of great importance to note that Tipα reduced the Young's modulus of MKN-1 cells determined by atomic force microscopy: This shows lower cell stiffness and increased cell motility. The morphological changes induced in human gastric cancer cells by Tipα are significant phenotypes of EMT. This is the first report that Tipα is a new inducer of EMT, probably associated with tumor progression in human gastric carcinogenesis.

In 1889, Stephen Paget used a seed and soil hypothesis to explain nonrandom patterns of metastasis,[1] and this concept is of more scientific significance at the molecular level of cancer cells.[2] This hypothesis deals with both cancer cells and cancer microenvironment in the host. Various carcinogenic factors, including cytokines and chemokines, induce tumor promotion and progression of cancer cells, associated with transition to a metastatic state. A typical example is generally called the epithelial–mesenchymal transition (EMT)[3]: EMT is theoretically understood as acquisition by epithelial cells of the phenotype of mesenchymal cells, such as fibroblasts. For example, the cells shut down the expression of numerous epithelial cell markers, such as cytokeratins and E-cadherin, and induce the expression of mesenchymal proteins, including vimentin, fibronectin, N-cadherin and integrin. Thus, the cancer cells phenotypically are more likely to become mesenchymal cells associated with metastatic states, such as change of cell shape and gene expression, acquisition of cell motility and local invasiveness into adjacent normal tissue.[4] Weinberg and coworkers intensively studied the changes in cell phenotype between EMT and mesenchymal–epithelial transition (MET), and reported that EMT is induced in epithelial cells by a diverse set of stimuli that include tumor growth factor-β (TGF-β), hepatocyte growth factor (HGF), tumor necrosis factor-α (TNF-α), hypoxia inducible factor 1α (HIF1α), and several transcription factors.[5] The early metastatic states of cancer cells are determined experimentally by migration, morphological changes and cell stiffness, while cancer microenvironment induces a unique environment with a highly acidic area that is low in oxygen, resulting in easier adaptation of cancer cells to microenvironment in the host.[6]

Key words: cell motility, filopodia, gastric cancer, nucleolin, Tipα
Abbreviations: AFM: atomic force microscopy; EMT: epithelial–mesenchymal transition; ERK: extracellular signal-regulated kinase; *H. pylori*: *Helicobacter pylori*; MEK: mitogen-activated protein kinase/extracellular signal-regulated kinase kinase; NF-κB: nuclear factor kappa-light-chain-enhancer of activated B cells; Tipα: TNF-α-inducing protein; TNF-α: tumor necrosis factor-α
Additional Supporting Information may be found in the online version of this article
Grant sponsors: Japan Society for the Promotion of Science, Smoking Research Foundation, Tokushima Bunri University, The Urakami Foundation
DOI: 10.1002/ijc.28582
History: Received 22 Apr 2013; Accepted 22 Oct 2013; Online 6 Nov 2013
Correspondence to: Masami Suganuma, PhD, Ina, Kitaadachi-gun, Saitama 362-0806, Japan, Tel.: +81-48-722-1111, ext. 4611, Fax: +81-48-722-1739, E-mail: masami@cancer-c.pref.saitama.jp

What's new?

Helicobacter pylori **strains are known to produce TNF-α inducing protein (Tipα) as a carcinogenic factor in the gastric epithelium. Here the authors sought to understand the underlying mechanisms of tumor progression. They demonstrated that Tipα induces migration, elongation, and filopodia of human gastric cancer cell lines. Tipα, which decreases cell stiffness, also enhances phosphorylation of cancer-related proteins, and increases the expression of vimentin with activation of MEK-ERK signal cascade. This is the first report that Tipα is a new inducer of epithelial-mesenchymal transition, probably associated with tumor progression in human gastric carcinogenesis.**

Our study of gastric carcinogenesis began with the finding of a new carcinogenic and inflammatory factor, TNF-α-inducing protein (Tipα) of *Helicobacter pylori* (*H. pylori*). The *Tipα* gene was cloned from a genome sequence of *H. pylori* strain 26695, and Tipα protein consists of 172 amino acids with 19 kDa; it acts as a homodimer with 38 kDa and is a strong TNF-α inducer.[7] A deletion mutant of Tipα (del-Tipα) lacking the N-terminal six amino acids, including two cysteines, is an inactive monomer that was used in our experiments as a negative control.[7] Clinical isolates of *H. pylori* from gastric cancer patients secrete much more Tipα protein than those from gastritis patients, suggesting that Tipα causes inflammation related to carcinogenesis.[8] On the basis of our evidence that Tipα induces *TNF-α* gene expression and transforms Bhas 42 cells (v-H-*ras*-transfected BALB/3T3 cells),[7] we concluded that Tipα is a new tumor promoter of *H. pylori*. We recently demonstrated that nucleolin is located on cell surface (surface nucleolin) in human and mouse gastric cancer cell lines, and is a receptor of Tipα[9,10] Surface nucleolin shuttles Tipα from membrane to the nuclei resulting in *TNF-α* gene expression through the activation of NF-κB (nuclear factor kappa-light-chain-enhancer of activated B cells) in both human and mouse cancer cell lines. As nuclear nucleolin is known to be as a DNA-, RNA- and protein-binding protein in the nucleolus, nucleolin regulates DNA and RNA metabolism in nuclei, and modulates various gene expressions by binding to mRNA in cytosol.[11,12] Thus, both surface and nuclear nucleolins have multifunctions that depend on different localizations in the cells. Surface nucleolin is glycosylated,[13] acts as a receptor for several ligands, is involved in signal transduction on the cell surface[14] and is constantly induced in proliferating tumor cells.[15]

As treatment of a human gastric cancer cell line with *H. pylori* is reported to induce cytoskeletal reorganization through activation of Rac[16] and phosphorylation of focal adhesion kinase (FAK),[17] *H. pylori* infection appears to act as an inducer of cell adhesion and motility. However, it is not yet known precisely which particular molecule of *H. pylori* induces phenotypes of EMT in the cells, specifically the metastatic states. In light of evidence that Tipα induces both NF-κB activation and TNF-α protein expression,[7] which are already known to be EMT inducers,[18] we studied whether Tipα might be a new EMT inducer for gastric cancer cells. Gastric cancer causes metastasis mainly in adjacent normal tissues, such as lymph nodes, peritoneum, and liver. To study the EMT-inducing activity of Tipα, we confirmed the phenotypic changes in human gastric cancer cell lines induced by Tipα. This is the first report to show that Tipα induces migration, morphological changes with filopodia, reduces cell stiffness, phosphorylates cancer-related proteins and increases expression of vimentin, mediated through phosphorylation of MEK-ERK proteins in human gastric cancer cell lines. We previously reported that the stiffness of mouse B16 melanoma subclones determined by atomic force microscopy (AFM) is closely correlated with their cell motility.[19] In addition, it has been reported that metastatic cancer cells isolated from the body fluids of patients with lung, breast and pancreatic cancers showed lower cell stiffness than normal mesothelial cells obtained from those body fluids.[20] This article presents significant results. Treatment of a human gastric cancer cell line with Tipα decreases cell stiffness, associated with a lower Young's modulus and higher cell motility. We report here that Tipα is a new inducer of EMT in human gastric cancer cell lines, and that it may stimulate tumor progression.

Material and Methods

Cell culture and reagents

Four human gastric cancer cell lines were purchased from RIKEN BRC Cell Bank (Ibaraki, Japan), American Type Culture Collection (Manassas, VA) and Immuno-Biological Laboratories (Gunma, Japan): MKN-1 (adenosquamous cell carcinoma), AGS (adenocarcinoma), MKN-7 (well-differentiated tubular adenocarcinoma) and MKN-28 (moderately differentiated tubular adenocarcinoma). The cell lines were grown in RPMI 1640 medium (NISSUI, Tokyo, Japan) with 10% fetal bovine serum (FBS) (JRH Bioscience, KS) at 37°C under 5% CO_2. Anti-nucleolin antibody (Anti-NUC295) and TNF-α were kindly provided by Dr. Kazuya Hirano (Tokyo University of Pharmacy and Life Science)[21] and Asahi Chemical Industry. Antibodies against actin, lamin B and vimentin were purchased from Santa Cruz Biotechnology (Santa Cruz, CA). Antibodies against epidermal growth factor receptor (EGFR), MEK1, phospho-MEK1 (Ser 217/Ser 221), ERK1/2 and phospho-ERK1/2 (Thr 202/Tyr 204) were purchased from Cell Signaling (Palo Alto, CA). AS1411 with the sequence 5′-d(GGTGGTGGTGGTTGTGGTGGTGGTGG)-3′ and a control for AS1411, cytosine-rich oligonucleotide (CRO) with the sequence 5′-d(CCTCCTCCTCCTTCTCCTC

CTCCTCC)-3′, were synthesized by Sigma Aldrich (Tokyo, Japan). Lactoferrin was purchased from Sigma Aldrich.

Preparation of recombinant Tipα and del-Tipα

His-tagged Tipα and His-tagged del-Tipα proteins were expressed in *Escherichia coli* (DE3) transformed by pET28a(+) vector containing *Tipα* or *del-Tipα* genes. Recombinant Tipα protein and recombinant del-Tipα, a deletion mutant of Tipα, were obtained with Ni-chelating resin, as described previously.[7] Both proteins were more than 98% pure for sodium dodecyl sulfate-polyacrylamide gel electrophoresis (SDS-PAGE).

Migration of gastric cancer cells by Transwell assay

The migration of human gastric cancer cell lines was assayed using a Transwell cell culture chamber (Becton-Dickinson, NJ), as described previously.[19] Cells (1×10^4/100 μl) in serum-free RPMI 1640 containing 0.1% bovine serum albumin (BSA) were seeded onto the insert well with an 8-μm-pore filter. Tipα (50 or 100 μg/ml), del-Tipα (50 or 100 μg/ml) or TNF-α (50 or 100 ng/ml) was added to a lower chamber containing serum-free RPMI 1640 medium and then kept for 24 hr at 37°C; 10% FBS and fibronectin (10 μg/ml) were used as positive controls in the same experimental conditions. The cells that migrated to the reverse side of the filter were stained with trypan blue and then photographed in 200× magnification. Migration was expressed as the number of migrated cells counted in three different areas on each membrane.

MKN-1 cells treated with various concentrations of AS1411 (nucleolin-targeted DNA aptamer), CRO (a negative control of AS1411) or lactoferrin were seeded in the upper chambers, and incubated with 100 μg/ml Tipα in a lower chamber for 24 hr. Inhibitory effects of AS1411 and lactoferrin on Tipα-induced migration were expressed as % of control. The results are the mean of three to six independent experiments.

Knockdown of nucleolin in MKN-1 cells by small interfering RNA

Nucleolin-targeted small interfering RNAs (siRNA-n1 and siRNA-n2) were purchased from Santa Cruz Biotechnology and Origene (Rockville, MD). siRNA-n1 is a mixture of three siRNAs with different nucleotide sequences, and siRNA-n2 has a single nucleotide sequence. A negative control (siRNA-nc) was purchased from Santa Cruz Biotechnology. The sequence of the nucleotides was not provided by the company. siRNA oligoduplexes at a final concentration of 10 nM were transfected into MKN-1 cells, which were plated at a density of 2.5×10^5 cells in RPMI 1640 containing 10% FBS, using Lipofectamine RNAiMAX Reagents (Invitrogen, CA). After incubation for 48 hr, MKN-1 cells were subjected to Transwell assay and examination of cell morphology.

Subcellular fractionation

After incubation of MKN-1 cells with each siRNA for 48 hr, homogenates of the cells were fractionated into membrane, cytosol and nuclei using Qproteome cell compartment kit (Qiagen, Düsseldorf, Germany), according to the manufacturer's instructions. Each fraction was subjected to Western blotting, using anti-nucleolin, anti-HSP90 (a marker for cytosol), anti-EGFR (for membrane) and anti-lamin B antibodies (for nuclei).

Western blotting

MKN-1 cells were lysed with lysis buffer containing 20 mM Tris-HCl (pH 8.0), 150 mM NaCl, 1% Triton X-100, 0.1% SDS, 1% sodium deoxycholate, 10 μg/ml aprotinin, 10 μg/ml leupeptin, 1 mM phenylmethanesulfonyl fluoride (PMSF), 5 mM sodium fluoride, 12 mM glycerol-6-phosphate, 2.5 mM sodium pyrophosphate and 1 mM sodium orthocarbonate. The cell lysates were subjected to SDS-PAGE and then transferred onto nitrocellulose membranes by electric blotting. The membranes were blocked with 3% skim milk in 20 mM Tris-HCl (pH 7.6) and 150 mM NaCl with 0.1% Tween 20, and then incubated with the indicated primary antibody. Bound antibodies were detected using horseradish peroxidase-conjugated secondary antibodies with Enhanced ChemiLuminescence (ECL) system (GE Healthcare, UK).

Cell morphology

MKN-1 cells (2.5×10^5 cells/500 μl) were cultured in serum-free RPMI 1640 with 100 μg/ml Tipα or del-Tipα in 24-well plates. The elongated cells and spherical cells were observed in 100× magnification after incubation at 37°C for 1–12 hr. MKN-1 cells treated with siRNA for 48 hr were cultured in serum-free RPMI 1640 containing 25 μg/ml Tipα. The elongated cells and spherical cells were counted separately. Total number of counted cells was about 500 in each condition, and the values are the means of two independent experiments.

Staining of actin filaments with phalloidin

MKN-1 cells were treated with 100 μg/ml Tipα, 10% FBS or 10 μg/ml fibronectin on the coverglass plates overnight in serum-free RPMI 1640 at 37°C and then washed with PBS. The cells were fixed with 4% paraformaldehyde and then permeabilized with 0.1% Triton X-100. After blocking with Image-iT™ FX Signal Enhancer (Invitrogen), the cells were stained with Alexa Fluor 488-conjugated phalloidin (Invitrogen) and propidium iodide, and then observed using fluorescence microscopy (Leica, Wetzlar, Germany).

Cell stiffness by AFM

Cell stiffness was measured using MFP-3D-BioJ-AFM (Asylum Research, CA) with a sharpened silicon nitride cantilever (TR400PSA 0.02N/m of spring constant, Olympus, Tokyo, Japan), as reported previously,[19] with some modifications. Force curves were recorded at 0.5 Hz for determination of Young's modulus (*E*, Pa). *E* value was calculated by fitting with Hertz model. The Poisson ratio of the cells was taken to be 0.5, as described previously.[22] The effects of 100 μg/ml

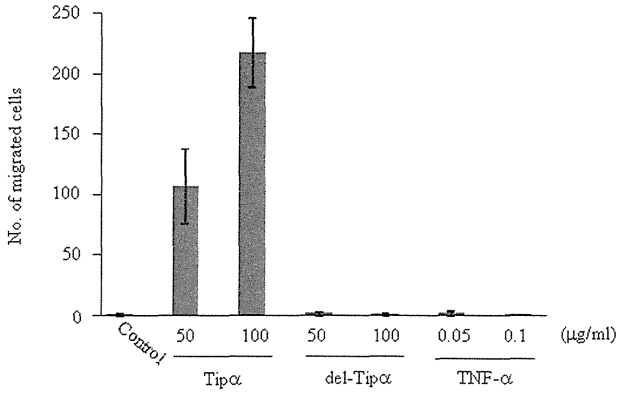

Figure 1. Migration of MKN-1 cells induced by Tipα. Tipα, del-Tipα and TNF-α were separately added in a lower chamber containing serum-free medium.

Tipα on stiffness of MKN-1 cells in serum-free RPMI 1640 were measured by AFM 24 hr after incubation, and the mean values of Young's modulus were obtained from log-normal fitting curves.

Phosphorylation of cancer-related proteins in MKN-1 cells treated with Tipα

MKN-1 cells were cultured in serum-free RPMI 1640 with or without 100 μg/ml Tipα, 15 min after incubation at 37°C, and the cell extracts were then subjected to analysis using Cancer Signaling Phospho Antibody Array (Filgen, Nagoya, Japan). Phosphorylation of 89 cancer-related proteins was examined using Chip spotted with a total of 248 phosphorylation-site-specific antibodies. Eleven proteins were found in the twofold difference of phosphorylated signal between Tipα-treated cells and nontreated cells.

Statistical analysis

Migration was analyzed by the two-sample independent Student's *t*-test, and the difference in mean values for Young's modulus was conducted using nonparametric analysis with Wilcoxon–Mann–Whitney test. The $p < 0.05$ was estimated to be significant.

Results

Migration of human gastric cancer cell lines by Tipα

The migration of human gastric cancer cell line MKN-1 treated with Tipα was dose-dependently induced in serum-free condition, as determined by Transwell assay: it was not induced by del-Tipα an inactive Tipα (Fig. 1). Table 1 shows the migrated cell numbers of four human gastric cancer cell lines, MKN-1, AGS, MKN-7 and MKN-28, induced by Tipα and three other inducers, TNF-α, FBS and fibronectin. The order of migration potency by Tipα was MKN-1 > AGS > MKN-7 = MKN-28. MKN-1 cell line (adenosquamous cell carcinoma) showed the strongest migration among the four examined gastric cancer cell lines (Table 1). Although Tipα induces the secretion of TNF-α from gastric cancer cells, the migration was not directly induced by TNF-α in the same experimental conditions.

Table 1. Migration of human gastric cancer cell lines by Tipα compared with TNF-α, FBS and fibronectin

	No. of migrated cells ± SD				
Cell lines	Control	Tipα	TNF-α	FBS	Fibronectin
MKN-1	1 ± 1	218 ± 28	1 ± 1	68 ± 26	49 ± 17
AGS	0	54 ± 9	2 ± 4	6 ± 2	3 ± 2
MKN-7	0	38 ± 19	0	1 ± 1	50 ± 27
MKN-28	0	38 ± 15	0	39 ± 6	16 ± 5

The migration was induced by treatment with 100 μg/ml Tipα, 50 ng/ml TNF-α, 10% FBS or 10 μg/ml fibronectin in serum-free medium for 24 hr, respectively.

Role of nucleolin in migration of MKN-1 cells induced by Tipα

Next, we studied the role of surface nucleolin in the migration induced by Tipα. Treatment with nucleolin-targeted siRNA-n1 and siRNA-n2 reduced the amount of nucleolin in whole cell lysate to 50%, but negative control siRNA-nc did not reduce it (Fig. 2*a*). Treatment with siRNA-n1 and siRNA-n2 strongly downregulated surface nucleolin in the membrane fraction compared with that in the cytosol and nuclear fractions (Fig. 2*b*). We next studied the effects of nucleolin knockdown by siRNAs on migration of MKN-1 cells induced by Tipα. Treatment with siRNA-n1 and siRNA-n2 resulted in decreases of 60.4 and 86.1%, respectively (Fig. 2*c*), while the migration of MKN-1 cells induced by FBS was only slightly reduced by siRNA-n1, a decrease of 22.0% (Fig. 2*d*), and that induced by fibronectin was inhibited by only 5.0% (Fig. 2*e*). Control siRNA-nc did not inhibit the migration of MKN-1 cells induced by Tipα, FBS or fibronectin. The results suggest that surface nucleolin plays a key role in migration of gastric cancer cells induced by Tipα, and that the migration induced by FBS or fibronectin was mediated through different pathways than that of Tipα.

On the basis of evidence that AS1411 is a nucleolin-targeted DNA aptamer,[23] and that lactoferrin interacts with cell surface nucleolin,[24] we studied whether nucleolin-binding molecules, such as AS1411 and lactoferrin, inhibit the migration of MKN-1 cells induced by Tipα: AS1411 dose-dependently inhibited the migration of MKN-1 cells, and 10 μM AS1411 caused a 53.9% reduction, whereas the control oligonucleotide of AS1411 (CRO) only slightly inhibited the migration (Fig. 2*f*). In addition, lactoferrin dose-dependently inhibited the migration of MKN-1 cells induced by Tipα, and treatment with 50 μg/ml lactoferrin completely inhibited it (Fig. 2*f*). However, lactoferrin did not inhibit migration of MKN-1 cells induced by fibronectin (data not shown). As AS1411 and lactoferrin are known to be incorporated into the cells through surface nucleolin, the results confirm that surface nucleolin induces cell migration by Tipα.

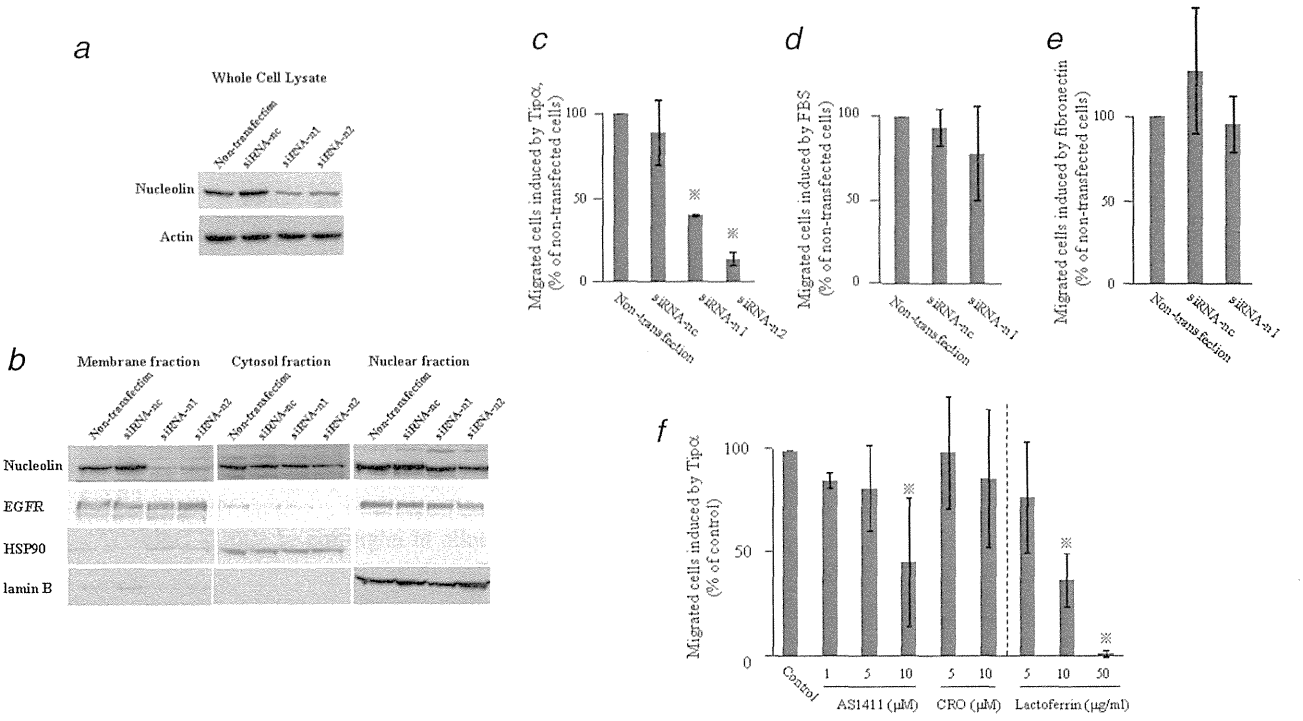

Figure 2. Inhibition of cell migration in MKN-1 cells by nucleolin-targeted siRNAs and nucleolin-binding molecules. (*a*) The expression of nucleolin was affected by nontransfection, control siRNA-nc and two different nucleolin-targeted siRNA-n1 and siRNA-n2. (*b*) The expression of nucleolin in the membrane fraction was downregulated by siRNA-n1 and siRNA-n2. (*c*) Migration of MKN-1 cells induced by Tipα. The cells were previously treated with nontransfection, control siRNA-nc, siRNA-n1 and siRNA-n2. (*d*) Migration of MKN-1 cells induced by FBS. The cells were previously treated with nontransfection, control siRNA-nc and siRNA-n1. (*e*) Migration of MKN-1 cells induced by fibronectin. The cells were previously treated with nontransfection, control siRNA-nc and siRNA-n1. (*f*) Migration of MKN-1 cells induced by Tipα in the presence of AS1411, CRO and lactoferrin. All the values are expressed as the average of three independent experiments with SD value, $*p < 0.05$.

Elongation of MKN-1 cells induced by Tipα

During our study on the migration of MKN-1 cells, we found that Tipα in a lower chamber induced cell attachment to the Transwell membrane and elongation of the cells on that membrane. To characterize the nature of cell elongation induced by Tipα, MKN-1 cells were treated with 100 μg/ml Tipα or del-Tipα in serum-free medium. When MKN-1 cells were cultured in serum-free medium, most cells maintained their spherical form (control) even 3 hr after seeding (Fig. 3*a*). However, treatment with Tipα began to elongate the morphology of the cells only 1 hr later. The number of elongated cells increased time-dependently, with most of the cells elongated within 3 hr after treatment, and remaining elongated until 12 hr after (Fig. 3*a*). Treatment with del-Tipα did not induce any elongation of the cells nor did control (Fig. 3*a*). The results show that Tipα induces the elongation of MKN-1 cells, and suggest that the morphological changes are associated with induction of cell migration and early invasiveness.

The role of nucleolin in the elongation of MKN-1 cells was next studied. Knockdown of nucleolin by siRNA-n1 and siRNA-n2 inhibited the elongation induced by Tipα, but siRNA-nc did not (Fig. 3*b*). Based on results showing that the number of elongated MKN-1 cells induced by Tipα was 60.8%, inhibition was 5.0, 16.5 and 39.1% by treatment with siRNA-nc, siRNA-n1 and siRNA-n2, respectively (Fig. 3*b*). The results suggest that the elongation of the cells induced by Tipα is mediated through the binding of Tipα to surface nucleolin.

Induction of filopodia in MKN-1 cells by Tipα

To characterize the morphological changes of MKN-1 cells induced by Tipα, actin filaments of MKN-1 cells were stained with Alexa Fluor 488-conjugated phalloidin 24 hr after seeding. We found that the filaments of elongated MKN-1 cells contain actin, which has a highly invasive structure (Fig. 3*c*). Figure 3*c* shows filamentous actin located around the cell surface, indicating that filopodia is induced in the cells. Although other treatments with FBS and fibronectin induced elongation of the cells in serum-free media, they did not induce filopodia (Fig. 3*c*). Thus, we believe that Tipα specifically induces filopodia, associated with migration of gastric cancer cells to extracellular environment.

Decrease in cell stiffness of MKN-1 cells by Tipα

We will also discuss cell stiffness of MKN-1 cells, based on our results showing that cell stiffness measured by AFM

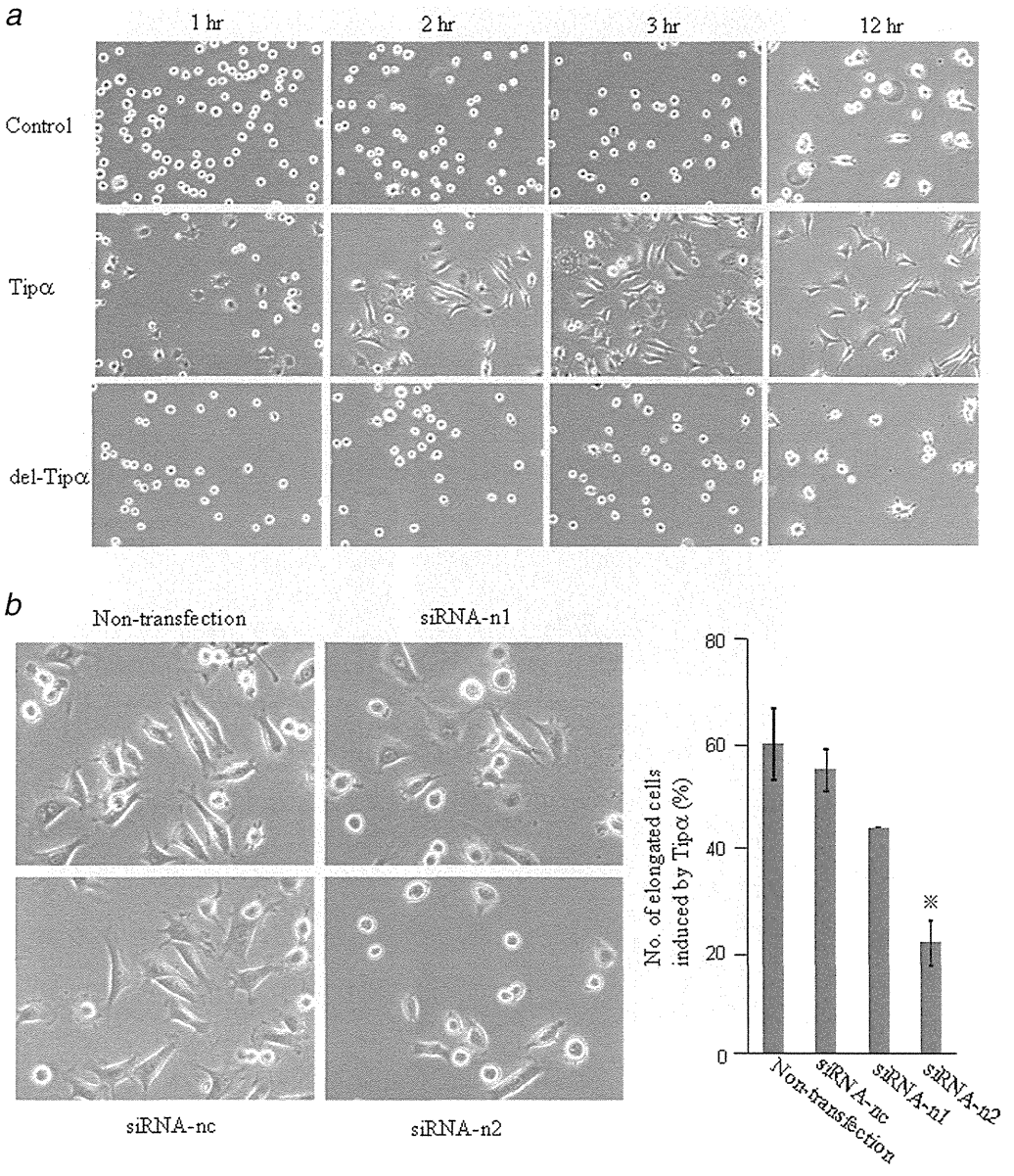

Figure 3. Morphological changes in MKN-1 cells induced by Tipα. (*a*) Elongation of MKN-1 cells time-dependently induced by Tipα but not del-Tipα. (*b*) Elongation of MKN-1 cells induced with Tipα by pretreatment with nontransfection, siRNA-nc, siRNA-n1 and siRNA-n2. The values are expressed as the average of two independent experiments with SD value, $*p < 0.05$. (*c*) Formation of filopodia in MKN-1 cells induced by Tipα. MKN-1 cells were treated with Tipα, FBS and fibronectin in serum-free medium and then stained with Alexa Fluor 488-conjugated phalloidin.

correlates well with the motility of cancer cells,[19] indicated by Young's modulus. Changes in cell stiffness of MKN-1 cells were studied by treatment with Tipα in serum-free medium. Young's modulus of the nontreated cells was 2,703 Pa, and that of Tipα-treated cells after 24 hr was 2,065 Pa, based on determination of about 600 force curves from 60 cells (Fig. 4). The reduction of Young's modulus by Tipα resulted in lower cell stiffness, *i.e.*, higher cell motility, than that of control. The report shows that Tipα reduced cell stiffness of MKN-1 cells and induced high cell motility.

Phosphorylation of cancer-related proteins in MKN-1 cells by Tipα

We presented results showing that MKN-1 cells treated with Tipα induce migration, elongation, formation of filopodia and decrease in cell stiffness, which are all related to phenotypic changes of EMT. To understand the molecular mechanism of such phenotypic changes, which occur in the cells within 1 hr after treatment with Tipα, we studied protein phosphorylation in MKN-1 cells as a quick response to Tipα. Analysis of 89 cancer-related proteins examined by The

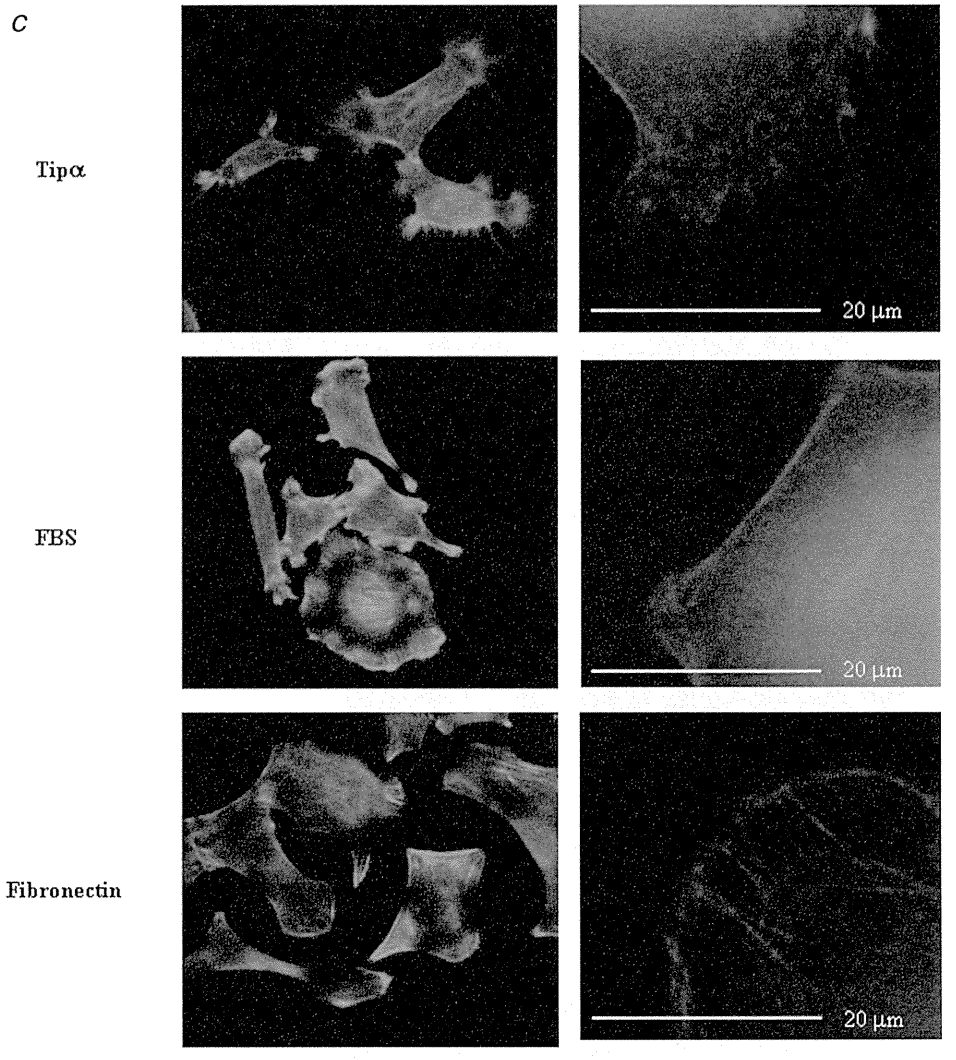

Figure 3. (Continued)

Cancer Signaling Phospho Antibody Array revealed that Tipα induces phosphorylation of 11 cancer-related proteins at the regulatory active sites more than twofold (Supporting Information Table 1). Furthermore, the phosphorylation of IκBα in MKN-1 cells increased about twofold after treatment with Tipα (data not shown); the results of which were the same as in our previous report.[7] As the MEK-ERK1/2 pathway is reported to be an important signal axis for induction of EMT,[25] and as it is activated by surface nucleolin,[26] we further confirmed by Western blotting that Tipα stimulated phosphorylation at Ser217/Ser221 of MEK1 and at Thr202/Tyr204 of ERK1/2 (Fig. 5*a*). These results show that Tipα stimulates the MEK/ERK1/2 signaling pathway, associated with phenotypic changes in EMT.

Protein expression in MKN-1 cells by Tipα

Looking at induction of EMT, we found that MKN-1 cells slightly express N-cadherin and vimentin but not E-cadherin (data not shown) in the nontreated state. Treatment of MKN-1 cells with Tipα enhanced the expression of vimentin, an intermediate filament of the mesenchymal cell cytoskeleton, and the expression reached maximal levels 3–6 hr later, before returning to basal level (Fig. 5*b*). The results suggest that Tipα acts as an inducer of EMT in gastric cancer cell line MKN-1, and that Tipα induces malignant phenotypes in human gastric cancer.

Discussion

Our study on Tipα, a carcinogenic factor secreted from *H. pylori*, has significantly extended our understanding of *H. pylori* carcinogenesis in humans. Specifically, Tipα first binds to surface nucleolin in human gastric cancer cells, and the complex is rapidly internalized into the cells. The signal transduction induces expression of *TNF-α* gene through the activation of NF-κB, resulting in tumor promotion and

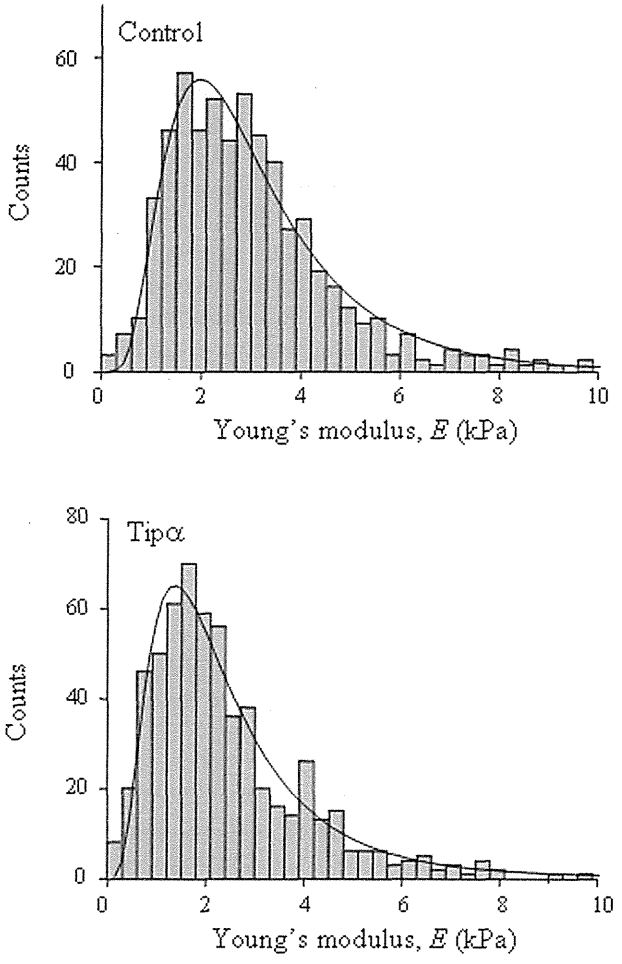

Figure 4. Histogram of Young's modulus obtained from force curve of MKN-1 cells after treatment with Tipα. Decrease in cell stiffness of MKN-1 cells was shown by treatment with Tipα.

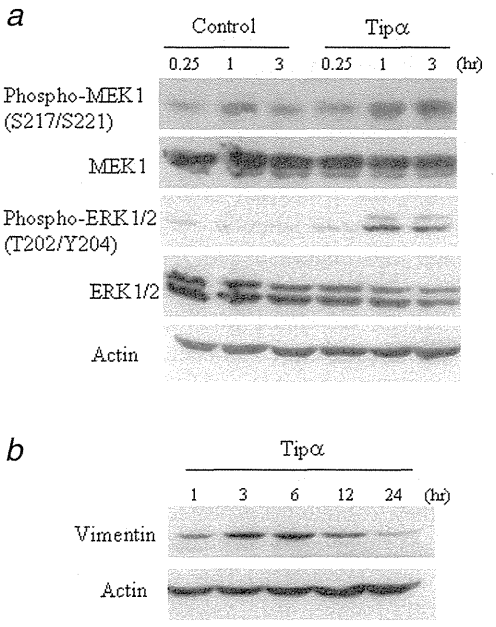

Figure 5. Increased phosphorylation of MEK1 and ERK1/2 induced by Tipα (*a*) and induction of vimentin expression in MKN-1 cells by Tipα (*b*).

progression.[7,9,10] In addition, we previously reported that Tipα induces *chemokine* gene expression, including Ccl2, Ccl7, Ccl20, Cxcl1, Cxcl2, Cxcl5 and Cxcl10,[27] which further suggests that the induction of Cxcl1 and Cxcl5 by TNF-α results in metastasis.[28] All the results show that Tipα induces tumor progression of *H. pylori* gastric carcinogenesis in humans.[29] This is well supported by evidence that HB-19 pseudopeptide binding to surface nucleolin induces rapid and intense membrane Ca^{2+} fluxes in various types of cells.[14]

This article presents results showing that treatment of gastric cancer cell line MKN-1 with Tipα induced numerous cellular effects: migration, elongation, formation of filopodia, decrease in cell stiffness associated with enhanced cell motility, phosphorylation of cancer-related proteins and expression of vimentin; all of these are phenotypic changes accompanying EMT. The formation of filopodia was induced only in the cells treated with Tipα, and because filopodia is an important marker of partial or complete EMT in human gastric cancer cells, we anticipate demonstrating that Tipα induces cancer metastasis in rodents. In other studies, we have presented the results on cell stiffness. Tipα reduced cell stiffness in human gastric cancer cells and contributed to an increase in cell motility. As cell stiffness is often discussed in relation to reorganization of actin filaments[30] and adhesion molecules,[31] it will be worthwhile to investigate cytoskeletal changes using high-resolution imaging to show how Tipα decreases cell stiffness. Migration and elongation of the cells were induced within 1–3 hr after treatment with Tipα, and phosphorylation of 11 proteins, including MEK1 and ERK1/2, was found as associated results of the signal transduction. The results show that activation of MEK and ERK1/2 pathway through surface nucleolin is involved in the EMT induction by Tipα. The precise relationship between MEK and ERK1/2 pathway and the induction of Ca^{2+} membrane fluxes remains to be studied.

It is a unique feature of *H. pylori* survives that it is in the acidic environment of gastric epithelium. Recently, a study on the structure of the proton-gated urea inner-membrane urea channel (*Hp*Urel) of *H. pylori* revealed the region of urea entry. *Hp*Urel closes at pH 7.0 and fully opens at pH 5.0 to allow the rapid access of urea to cytoplasmic urease.[32] We previously elucidated the crystal structure of del-Tipα, which has a heart-shaped homodimer *via* noncovalent bonds, which is assumed to be very similar to Tipα homodimer.[33] The crystal structure of del-Tipα contains a flexible region, so the activity of Tipα-inducing EMT will be affected by environmental pH.

We will briefly discuss here the significance of nucleolin in *H. pylori* carcinogenesis in humans. The migration and elongation of MKN-1 cells induced by Tipα, mediated

through the binding to surface nucleolin, were inhibited by treatment with siRNA-n1 and siRNA-n2, suggesting that phenotypic changes in EMT will be inhibited by siRNAs. Nucleolin has various binding molecules, such as AS1411,[23] HB-19 pseudopeptide,[34] lactoferrin,[24] midkine,[35] EGFR,[36,37] H-Ras, K-Ras[38] and endostatin.[39] HB-19 pseudopeptide inhibits migration of human umbilical vein epithelial cell (HUVEC), resulting in inhibition of angiogenesis.[26] Furthermore, cancer cell migration and metastasis of spontaneous melanoma in RET mice were inhibited by pseudopeptides including HB-19, associated with reduction of MMP-2 and MMP-9.[40–42] Thus, surface nucleolin plays a specific role in regulating cancer progression.

Several EMT inducers, including TGF-β, TNF-α and HGF, have been reported, and TGF-β induces EMT 48–72 hr after treatment.[43] Although the inducers have numerous functions, they commonly activate the NF-κB pathway in epithelial cells, suggesting that the induction of EMT is linked to tumor promotion. This study revealed that Tipα acts as an EMT inducer of *H. pylori*.

Recently, some transcription factors have been shown to be EMT regulators, Snail and Slug, which are repressors of E-cadherin, Twist, an activator of N-cadherin during *Drosophila* embryogenesis, and FOXc2.[4] *H. pylori* infection increases expression of *Snail, Slug* and *vimentin* genes in gastric cancer cells.[44] Rosivatz *et al.* studied the expression of *Snail, SIP1, Twist, E-cadherin* and *N-cadherin* genes in 28 diffuse-type and 20 intestinal-type human gastric cancers.[45] The tissues of diffuse-type showed reduction of E-cadherin by 39% and the upregulation of Snail, Twist and N-cadherin. On the other hand, the tissues of intestinal-type showed reduction of E-cadherin by 60%, associated with upregulation of SIP1 and downregulation of Snail, Twist and N-cadherin.[45] The results indicate that the roles of transcription factors are dependent on the histological phenotypes. Cancer cell line MKN45, derived from undifferentiated gastric cancer, expressed high levels of Twist, and downregulation of Twist inhibited cell migration and invasion, showing that Twist regulates cell migration and invasion in gastric cancer cells.[46] In this article, we did not find any downregulation of E-cadherin, as E-cadherin was only slightly expressed, and Snail and Zeb1 were expressed in the nontreated MKN-1 cells. Looking at the process of EMT, Tipα increased expression of vimentin 3–6 hr after treatment, associated with an increase in migration, formation of filodpodia and a decrease in cell stiffness. This article is the first to report a new function of Tipα, an EMT inducer of *H. pylori*.

Acknowledgements

The authors thank Drs. Kazuya Hirano and Masatoshi Beppu at Tokyo University of Pharmacy and Life Science for the supply of anti-nucleolin antibody (anti-NUC295), and Asahi Chemical Industry for the supply of TNF-α. They also thank Dr. Yoichi Tanaka at Saitama Cancer Center for his encouragement and fruitful discussion, and Ms. Ikuko Shiotani at the Research Institute for Clinical Oncology, Saitama Cancer Center for her technical assistance.

References

1. Paget S. The distribution of secondary growth in cancer of breast. *Lancet* 1889;133:571–3.
2. Fidler IJ. The pathogenesis of cancer metastasis: the 'seed and soil' hypothesis revisited. *Nat Rev Cancer* 2003;3:453–8.
3. Polyak K, Weinberg RA. Transitions between epithelial and mesenchymal states: acquisition of malignant and stem cell traits. *Nat Rev Cancer* 2009;9:265–73.
4. Weinberg RA. Moving out invasion and metastasis. In: Weinberg RA, ed. The biology of cancer. New York: Garland Science, Taylor & Francis Group LLC, 2007. 587–654.
5. Hanahan D, Weinberg RA. Hallmarks of cancer: the next generation. *Cell* 2011;144:646–74.
6. Marx V. Tracking metastasis and tricking cancer. *Nature* 2013;494:133–6.
7. Suganuma M, Kurusu M, Suzuki K, et al. New tumor necrosis factor-α-inducing protein released from *Helicobacter pylori* for gastric cancer progression. *J Cancer Res Clin Oncol* 2005;131:305–13.
8. Suganuma M, Yamaguchi K, Ono Y, et al. TNF-α-inducing protein, a carcinogenic factor secreted from *H. pylori*, enters gastric cancer cells. *Int J Cancer* 2008;123:117–22.
9. Watanabe T, Tsuge H, Imagawa T, et al. Nucleolin as cell surface receptor for tumor necrosis factor-α inducing protein: a carcinogenic factor of *Helicobacter pylori*. *J Cancer Res Clin Oncol* 2010;136:911–21.
10. Watanabe T, Hirano K, Takahashi A, et al. Nucleolin on the cell surface as a new molecular target for gastric cancer treatment. *Biol Pharm Bull* 2010;33:796–803.
11. Ginisty H, Sicard H, Roger B, et al. Structure and functions of nucleolin. *J Cell Sci* 1999;112:761–72.
12. Storck S, Shukla M, Dimitrov S, et al. Functions of the histone chaperone nucleolin in diseases. *Subcell Biochem* 2007;41:125–44.
13. Carpentier M, Morelle W, Coddeville B, et al. Nucleolin undergoes partial N- and O-glycosylations in the extranuclear cell compartment. *Biochemistry (Mosc)* 2005;44:5804–15.
14. Losfeld ME, Khoury DE, Mariot P, et al. The cell surface expressed nucleolin is a glycoprotein that triggers calcium entry into mammalian cells. *Exp Cell Res* 2009;315:357–69.
15. Hovanessian AG, Soundaramourty C, El Khoury D, et al. Surface expressed nucleolin is constantly induced in tumor cells to mediate calcium-dependent ligand internalization. *PLoS One* 2010; 5:e15787.
16. Palovuori R, Perttu A, Yan Y, et al. *Helicobacter pylori* induces formation of stress fibers and membrane ruffles in AGS cells by rac activation. *Biochem Biophys Res Commun* 2000; 269:247–53.
17. Tabassam FH, Graham DY, Yamaoka Y. OipA plays a role in *Helicobacter pylori*-induced focal adhesion kinase activation and cytoskeletal reorganization. *Cell Microbiol* 2008;10:1008–20.
18. Huber MA, Beug H, Wirth T. Epithelial-mesenchymal transition: NF-κB takes center stage. *Cell Cycle* 2004;3:1477–80.
19. Watanabe T, Kuramochi H, Takahashi A, et al. Higher cell stiffness indicating lower metastatic potential in B16 melanoma cell variants and in (-)-epigallocatechin gallate-treated cells. *J Cancer Res Clin Oncol* 2012;138:859–66.
20. Cross SE, Jin YS, Rao J, et al. Nanomechanical analysis of cells from cancer patients. *Nat Nanotechnol* 2007;2:780–3.
21. Hirano K, Miki Y, Hirai Y, et al. A multifunctional shuttling protein nucleolin is a macrophage receptor for apoptotic cells. *J Biol Chem* 2005; 280:39284–93.
22. Trickey WR, Baaijens FP, Laursen TA, et al. Determination of the Poisson's ratio of the cell: recovery properties of chondrocytes after release from complete micropipette aspiration. *J Biomech* 2006;39:78–87.
23. Ireson CR, Kelland LR. Discovery and development of anticancer aptamers. *Mol Cancer Ther* 2006;5:2957–62.
24. Legrand D, Vigie K, Said EA, et al. Surface nucleolin participates in both the binding and endocytosis of lactoferrin in target cells. *Eur J Biochem* 2004;271:303–17.
25. Wang ZL, Fan ZQ, Jiang HD, et al. Selective Cox-2 inhibitor celecoxib induces epithelial-mesenchymal transition in human lung cancer

cells via activating MEK-ERK signaling. *Carcinogenesis* 2013;34:638–46.
26. Destouches D, El Khoury D, Hamma-Kourbali Y, et al. Suppression of tumor growth and angiogenesis by a specific antagonist of the cell-surface expressed nucleolin. *PLoS One* 2008;3:e2518.
27. Kuzuhara T, Suganuma M, Kurusu M, et al. *Helicobacter pylori*-secreting protein Tipα is a potent inducer of chemokine gene expressions in stomach cancer cells. *J Cancer Res Clin Oncol* 2007; 133:287–96.
28. Acharyya S, Oskarsson T, Vanharanta S, et al. A CXCL1 paracrine network links cancer chemoresistance and metastasis. *Cell* 2012;150:165–78.
29. Fujiki H, Watanabe T, Suganuma M. Tumor promotion by TNF-α-inducing protein and its receptor nucleolin in human gastric carcinogenesis by *Helicobacter pylori*. *Trends Cancer Res* 2012;8:97–112.
30. Sharma S, Santiskulvong C, Bentolila LA, et al. Correlative nanomechanical profiling with super-resolution F-actin imaging reveals novel insights into mechanisms of cisplatin resistance in ovarian cancer cells. *Nanomedicine* 2012;8:757–66.
31. Docheva D, Padula D, Schieker M, et al. Effect of collagen I and fibronectin on the adhesion, elasticity and cytoskeletal organization of prostate cancer cells. *Biochem Biophys Res Commun* 2010; 402:361–6.
32. Strugatsky D, McNulty R, Munson K, et al. Structure of the proton-gated urea channel from the gastric pathogen *Helicobacter pylori*. *Nature* 2013; 493:255–8.
33. Tsuge H, Tsurumura T, Utsunomiya H, et al. Structural basis for the *Helicobacter pylori*-carcinogenic TNF-α-inducing protein. *Biochem Biophys Res Commun* 2009;388:193–8.
34. Nisole S, Krust B, Callebaut C, et al. The anti-HIV pseudopeptide HB-19 forms a complex with the cell-surface-expressed nucleolin independent of heparan sulfate proteoglycans. *J Biol Chem* 1999;274:27875–84.
35. Hovanessian AG. Midkine, a cytokine that inhibits HIV infection by binding to the cell surface expressed nucleolin. *Cell Res* 2006;16:174–81.
36. Farin K, Di Segni A, Mor A, et al. Structure-function analysis of nucleolin and ErbB receptors interactions. *PLoS One* 2009;4:e6128.
37. Farin K, Schokoroy S, Haklai R, et al. Oncogenic synergism between ErbB1, nucleolin, and mutant Ras. *Cancer Res* 2011;71:2140–51.
38. Inder KL, Lau C, Loo D, et al. Nucleophosmin and nucleolin regulate K-Ras plasma membrane interactions and MAPK signal transduction. *J Biol Chem* 2009;284:28410–19.
39. Shi H, Huang Y, Zhou H, et al. Nucleolin is a receptor that mediates antiangiogenic and antitumor activity of endostatin. *Blood* 2007;110:2899–906.
40. El Khoury D, Destouches D, Lengagne R, et al. Targeting surface nucleolin with a multivalent pseudopeptide delays development of spontaneous melanoma in RET transgenic mice. *BMC Cancer* 2010;10:325.
41. Krust B, El Khoury D, Soundaramourty C, et al. Suppression of tumorigenicity of rhabdoid tumor derived G401 cells by the multivalent HB-19 pseudopeptide that targets surface nucleolin. *Biochimie* 2011;93:426–33.
42. Krust B, El Khoury D, Nondier I, et al. Targeting surface nucleolin with multivalent HB-19 and related Nucant pseudopeptides results in distinct inhibitory mechanisms depending on the malignant tumor cell type. *BMC Cancer* 2011;11:333.
43. Larue L, Bellacosa A. Epithelial-mesenchymal transition in development and cancer: role of phosphatidylinositol 3′ kinase/AKT pathways. *Oncogene* 2005;24:7443–54.
44. Yin Y, Grabowska AM, Clarke PA, et al. *Helicobacter pylori* potentiates epithelial:mesenchymal transition in gastric cancer: links to soluble HB-EGF, gastrin and matrix metalloproteinase-7. *Gut* 2010;59:1037–45.
45. Rosivatz E, Becker I, Specht K, et al. Differential expression of the epithelial-mesenchymal transition regulators snail, SIP1, and twist in gastric cancer. *Am J Pathol* 2002;161:1881–91.
46. Yang Z, Zhang X, Gang H, et al. Up-regulation of gastric cancer cell invasion by Twist is accompanied by N-cadherin and fibronectin expression. *Biochem Biophys Res Commun* 2007;358:925–30.

Invest New Drugs (2014) 32:261–270
DOI 10.1007/s10637-013-9948-5

PHASE I STUDIES

Phase I study of sunitinib plus S-1 and cisplatin in Japanese patients with advanced or metastatic gastric cancer

Narikazu Boku · Kei Muro · Nozomu Machida · Satoshi Hashigaki · Nobuyuki Kimura · Mie Suzuki · Mariajose Lechuga · Yoshinori Miyata

Received: 28 November 2012 / Accepted: 1 March 2013 / Published online: 12 May 2013

Summary *Background* This phase I, dose-finding study evaluated the maximum tolerated dose (MTD), safety, pharmacokinetics, and antitumor activity of sunitinib plus S-1/cisplatin in Japanese patients with advanced/metastatic gastric cancer. *Patients and methods* Patients received oral sunitinib on a continuous daily dosing (CDD) or 2-weeks-on/2-weeks-off schedule (Schedule 2/2; 25 mg/day or 37.5 mg/day), plus S-1 (80–120 mg/day)/cisplatin 60 mg/m^2. *Results* Twenty-seven patients received treatment, including 26 patients treated per protocol (sunitinib 25 mg/day CDD schedule, $n=4$; sunitinib 25 mg/day Schedule 2/2, $n=16$ [dose-limiting toxicity (DLT) cohort, $n=6$ plus expansion cohort, $n=10$]; sunitinib 37.5 mg/day Schedule 2/2, $n=6$). One patient erroneously self-administered sunitinib 12.5 mg/day and was excluded from the analyses. The MTD was sunitinib 25 mg/day on Schedule 2/2. DLTs were reported for: 2/4 patients given sunitinib 25 mg/day on the CDD schedule; 1/6 patients administered sunitinib 25 mg/day on Schedule 2/2 (grade [G] 3 neutropenic infection, G4 thrombocytopenia, and S-1 dose interruption ≥5 days), and 3/6 patients given sunitinib 37.5 mg/day on Schedule 2/2. Results below are for the overall MTD cohort ($n=16$). The most frequently reported G3/4 adverse events were neutropenia (93.8 %) and leukopenia (75.0 %). The objective response rate was 37.5 %; six additional patients experienced no disease progression for ≥24 weeks. Median progression-free survival was 12.5 months. No pharmacokinetic drug–drug interactions were observed between sunitinib/S-1/cisplatin and S-1/cisplatin. *Conclusions* The MTD of sunitinib was 25 mg/day on Schedule 2/2 combined with cisplatin/S-1 in patients with advanced/metastatic gastric cancer. This regimen had a manageable safety profile and preliminary antitumor activity.

Keywords Sunitinib · Gastric cancer · Phase I · Dose-finding

Presented in part on the clinical trial registry located at ClinicalTrials.gov (identification No. NCT00553696) and at:

N. Boku (✉)
Department of Clinical Oncology, St. Marianna University School of Medicine, 2-16-1, Sugao, Miyamae-ku, Kawasaki, Kanagawa 216-8511, Japan
e-mail: n.boku@marianna-u.ac.jp

K. Muro
Department of Clinical Oncology, Aichi Cancer Center, Nagoya, Japan

N. Machida
Division of Gastrointestinal Oncology, Shizuoka Cancer Center, Shizuoka, Japan

S. Hashigaki
Clinical Statistics, Pfizer Japan, Tokyo, Japan

N. Kimura
Clinical Pharmacology, Pfizer Japan, Tokyo, Japan

M. Suzuki
Clinical Research, Pfizer Japan, Tokyo, Japan

M. Lechuga
Pfizer Oncology, Pfizer Italia Srl, Latina, Italy

Y. Miyata
Department of Oncology, Saku Central Hospital, Saku, Japan

Introduction

Gastric cancer is the second most common cause of cancer-related death worldwide, with more than 730,000 deaths estimated to have occurred in 2008 [1]. Globally, the

5-year survival rate for gastric cancer is approximately 20 % [2], and most patients present with advanced, non-resectable disease [3–5].

Despite recent advances in the treatment for gastric cancer [6], a standard chemotherapy regimen has not been established for recurrent or unresectable advanced gastric cancer; combination chemotherapy is associated with significant survival and quality of life advantages, compared with best supportive care [7, 8]. The use of a 5-fluorouracil (5-FU)-based regimen in combination with a platinum analog is the most widely accepted first-line treatment regimen, although combination therapy does have a higher associated toxicity burden compared with single-agent chemotherapy [8].

Blockade of receptors such as vascular endothelial growth factor receptor (VEGFR) and platelet-derived growth factor receptor (PDGFR) has been shown to inhibit tumor-related angiogenesis and tumor growth [9, 10]. Not only are these receptors expressed in gastric cancers but they are known to have direct effects on the growth and metastasis of this disease [9–14].

Sunitinib malate (SUTENT®; Pfizer Inc., New York, NY, USA) is an oral, multitargeted, tyrosine kinase inhibitor of VEGFRs 1–3, PDGFR-α and -β, and other receptors [15–17]. Sunitinib is approved multinationally for the treatment of unresectable and/or metastatic imatinib-resistant/-intolerant gastrointestinal stromal tumor, advanced/metastatic renal cell carcinoma, and unresectable or metastatic, well-differentiated pancreatic neuroendocrine tumors. Phase II study results in advanced gastric cancer have shown that sunitinib had activity as a single-agent; progression-free survival (PFS) was 2.3 months and overall survival was 6.8 months in the second-line setting [18].

In preclinical tumor models, sunitinib has been shown to enhance the antitumor activity of 5-FU and cisplatin, suggesting that sunitinib might enhance the effect of chemotherapy in cancer patients [19, 20]. In the First-Line Advanced Gastric Cancer Study (FLAGS), the combination of S-1, an oral derivative of 5-FU, and cisplatin was found to be effective when administered as a 3-week on/1-week off regimen (Schedule 3/1) [21]. Therefore, this phase I, dose-finding study was conducted to determine the maximum tolerated dose (MTD) and overall safety profile of sunitinib plus S-1 and cisplatin in Japanese patients with advanced/metastatic gastric cancer. Tolerability, pharmacokinetics (PK), and antitumor activity were also evaluated.

Materials and methods

Study population

Patients (male or female) eligible for inclusion in this study were aged ≥20 years, had an Eastern Cooperative Oncology Group performance status of 0 or 1, adequate organ function, and histologically or cytologically confirmed Stage IV gastric adenocarcinoma or gastroesophageal junction adenocarcinoma not amenable to surgery or radiation. Prior adjuvant therapy was permitted with a recurrence-free interval of >3 months after the completion of adjuvant therapy. Prior chemotherapy in the advanced/metastatic setting was not permitted; one regimen of chemotherapy, such as S-1 monotherapy, without progressive disease was allowed if the duration of treatment was less than 4 weeks.

Exclusion criteria included central nervous system (CNS) metastases, carcinomatous meningitis, or uncontrolled hypertension (blood pressure >150/100 mmHg). Patients with severe/unstable angina, myocardial infarction, coronary artery bypass graft, symptomatic congestive heart failure, cerebrovascular accident, including transient ischemic attack, or pulmonary embolism within 12 months prior to starting study treatment were also excluded.

The study was conducted in accordance with the International Conference on Harmonization Good Clinical Practice guidelines, the declaration of Helsinki, and applicable local regulatory requirements and laws. Approval from the institutional review board or independent ethics committee with the appropriate jurisdiction was required for each participating investigator/center. Written informed consent was obtained from all patients.

Study design

This was a phase I, open-label, dose-finding study of sunitinib in combination with S-1 and cisplatin in patients with advanced/metastatic gastric cancer (NCT00553696). Patients received open-label, oral S-1 at a starting dose of 80–120 mg/day (based on body surface area) on Schedule 3/1 and a cisplatin 60 mg/m^2 infusion on day 1 that was repeated every 28 days. Patients were allocated to different doses of oral sunitinib based on a 3+3 design. Initially, sunitinib was planned to be administered on a continuous daily dosing (CDD) schedule or on Schedule 3/1. After four patients received treatment in the CDD arm, the protocol was revised to use a 2-week-on/2-week-off schedule (Schedule 2/2), instead of Schedule 3/1, due to the pattern of adverse events (AEs). Patients received sunitinib 25 mg/day on a CDD schedule, or 25 mg/day or 37.5 mg/day on Schedule 2/2 in 4-week cycles (Fig. 1).

Initially, three patients were enrolled to receive sunitinib 25 mg/day on the CDD schedule in combination with S-1 and cisplatin 60 mg/m^2. If no patients experienced a dose-limiting toxicity (DLT) in cycle 1 then patients would be enrolled to the next highest dose level. If no more than one of the initial three patients experienced a DLT within cycle 1, then the cohort was expanded to a total of six patients. If no more than one of these six patients experienced a DLT,

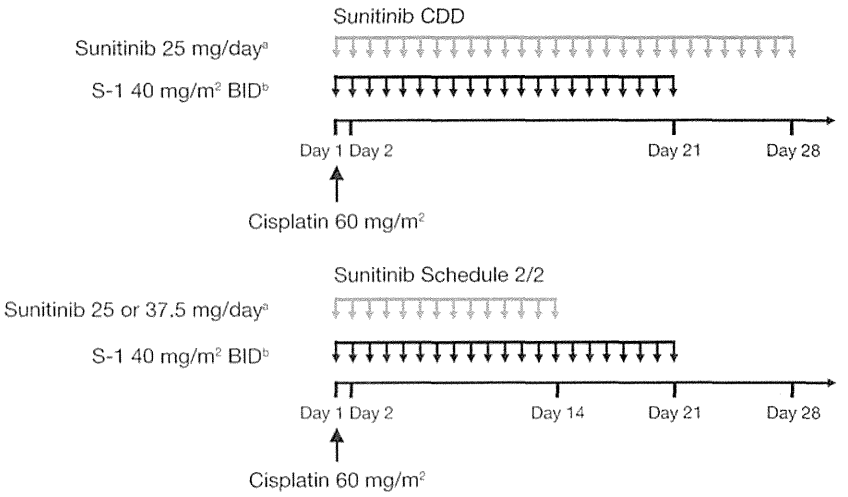

Fig. 1 Treatment schema. [a]Sunitinib dose withheld on cycle 1 day 1 to enable pharmacokinetic analysis of S-1 and cisplatin. [b]S-1 and cisplatin dose withheld on cycle 1 day 1 to enable pharmacokinetic analysis of sunitinib. *BID* twice daily; *Schedule 2/2* 2 weeks on treatment followed by 2 weeks off treatment

then patients would be enrolled at the next highest dose level.

The MTD was defined as the highest dose cohort where 0/3 or ≤1/6 patients experienced a DLT, with the next highest dose having at least 2/3 or 2/6 patients who experienced a DLT. DLTs are defined in Table 1. In this study, the MTD level was confirmed by expanding enrollment to include up to 10 additional patients with advanced/metastatic disease in order to obtain additional safety data for the combination treatment. It was anticipated that a total of approximately 30 patients would be enrolled in this study.

Dose modifications of sunitinib were not allowed until a DLT was reached. Once dose reduction occurred due to study drug-related toxicity, the dose was not re-escalated. Patients could undergo a maximum of two dose reductions of either S-1 and/or cisplatin. However, patients requiring more than two dose reductions of S-1 or sunitinib were withdrawn from the study. Additionally, patients with >1 missed cisplatin dose were withdrawn. Treatment was continued for 8 cycles or until disease progression, unacceptable toxicity, or withdrawal of patient consent.

The primary endpoint was the assessment of first-cycle DLTs for sunitinib plus S-1 and cisplatin. Secondary endpoints included overall safety, tumor response, PFS, and PK.

Assessments

Patients were evaluable for DLT assessment if they received all day 1 chemotherapy and ≥80 % of their sunitinib doses and S-1 doses. Those who could not receive ≥80 % of their doses for reasons other than a DLT were excluded from the DLT evaluation. Tumor assessment was performed at baseline, on day 22 of cycle 1, and every 4 weeks thereafter until radiographic-confirmed disease progression or end of treatment scan. Objective tumor response in patients with at least one target lesion was measured using the Response Evaluation Criteria in Solid Tumors (RECIST) guidelines [22]

Table 1 Definition of DLT

Category	DLT criteria
Hematologic	Grade 4 neutropenia lasting ≥7 days
	Grade ≥3 febrile neutropenia
	Grade ≥3 neutropenic infection
	Grade 4 thrombocytopenia or grade 3 thrombocytopenia with bleeding
Non-hematologic[a]	Grade 3 toxicities lasting ≥7 days
	Grade 4 non-hematologic toxicity
	Grade 3/4 nausea, vomiting or diarrhea persisting despite maximum supportive therapy
Missed/delayed dose due to toxicity	Break from sunitinib dose ≥6/28 days on the CDD schedule or ≥3/14 days on Schedule 2/2
	Break from S-1 dose ≥5/21 days per cycle
	Delay of >3 weeks in starting the second treatment cycle

CDD continuous daily dosing; *DLT* dose-limiting toxicity; *Schedule 2/2* 2 weeks on treatment followed by 2 weeks off treatment

[a] Exceptions: hyperamylasemia or hyperlipasemia without other clinical evidence of pancreatitis and asymptomatic hyperuricemia; asymptomatic hypertension with adequately controlled blood pressure

and confirmed no sooner than 4 weeks after the initial documentation of response.

Safety was assessed at regular intervals (during cycle 1 on days 1, 2, 8, 15, and 22; during cycles 2–8 on days 1, 2, and 21; and during cycles ≥9 on days 1 and 21). AEs were monitored during the study and graded using the National Cancer Institute Common Terminology for Adverse Events version 3.0 clinical assessments, including laboratory testing for blood hematology and serum chemistry.

To investigate PK drug–drug interactions, full PK profiles of sunitinib, its active metabolite SU12662, S-1 (5-FU, tegafur) and cisplatin (total and free) were assessed in all cohorts comprising the 3+3 design, and in the MTD expansion cohort. Blood samples for analyses of cisplatin and S-1 were collected on cycle 1 days 1–2 (S-1 and cisplatin), before starting sunitinib dosing on day 2, and on cycle 2 days 1–2 (in combination with sunitinib) in the MTD cohort. In the expansion cohort, blood samples for the analyses of sunitinib and SU12662 were collected on cycle 1 days 1–2 (sunitinib alone), prior to administration of S-1 and cisplatin on day 2, and cycle 2 days 1–2 (in combination with S-1 and cisplatin). PK parameters were calculated using non-compartmental methods.

Trough plasma concentrations of sunitinib and SU12662 were obtained at steady state on cycles 1–3 days 21–22 for the CDD schedule, and cycles 1–3 days 14–15 for Schedule 2/2. Blood samples were obtained before the administration of sunitinib and S-1.

On the day of cisplatin PK sampling, blood was drawn pre-dose (before administration of cisplatin, S-1 or sunitinib) and at 0.5, 1, 2, 8, and 22 h after completing infusion. Samples for evaluation of sunitinib, SU12662, and S-1 PK were obtained pre-dose (before administration of either S-1 or sunitinib) and at 1, 2, 4, 6, 8, and 10 h post-dose (before dosing of S-1). For sunitinib and SU12662, a sample was also obtained 24 h post-dose.

Plasma samples were analyzed for sunitinib and SU12662 concentrations by Bioanalytical Systems Inc. (USA) using a validated high-performance liquid chromatography tandem mass spectrometric (HPLC-MS/MS) method. Tegafur and 5-FU plasma concentrations were also determined using a validated HPLC-MS/MS method by Tandem Labs (USA). Cisplatin concentrations were determined in both plasma and plasma ultra filtrate samples by Covance Laboratories Inc. (USA) using a validated Inductively Coupled Plasma–Mass Spectrometric (ICP/MS) method.

Statistical analysis

The sample size was determined on an empirical rather than statistical basis. Assessment of 3–6 patients for each cohort was considered adequate to characterize the safety of a treatment regimen prior to investigation in phase II clinical trials. It was anticipated that up to 30 patients would be enrolled in this study.

Efficacy analyses included all patients who received at least one protocol-specified dose of sunitinib. Descriptive statistics were used to summarize all patient characteristics, treatment administration/compliance, antitumor activity, and safety; PFS was summarized using the Kaplan–Meier method. In an unplanned exploratory analysis, clinical benefit rate (CBR; percentage of patients with a complete response, partial response, and stable disease ≥24 weeks) and PFS were calculated in patients with scirrhous-type disease of primary tumors.

Results

Patient characteristics

In total, 27 patients received treatment, including 26 patients treated per protocol (sunitinib 25 mg/day on the CDD schedule, 4; sunitinib 25 mg/day on Schedule 2/2, 16 [DLT cohort, 6 plus expansion cohort, 10]; sunitinib 37.5 mg/day on Schedule 2/2, 6), and one patient who was assigned to sunitinib 25 mg/day on Schedule 2/2 and erroneously self-administered sunitinib 12.5 mg/day throughout the study. The latter patient was excluded from the efficacy analyses. One patient remained on study as of April 2012. Demographic and baseline disease characteristics are shown in Table 2. Overall, eight patients had scirrhous-type disease (seven patients in the MTD cohort).

Safety and drug exposure

Twenty-seven patients were evaluable for safety. The MTD was determined to be sunitinib 25 mg/day on Schedule 2/2 plus cisplatin and S-1, and a further 10 patients were allocated to this cohort. Of the four patients who received sunitinib 25 mg/day on the CDD schedule, two DLTs were reported: grade 4 thrombocytopenia ($n=1$), and grade 4 thrombocytopenia plus grade 3 febrile neutropenia ($n=1$). Subsequently, the treatment frequency was reduced to sunitinib 25 mg/day on Schedule 2/2. In the second cohort, one of six patients reported a DLT: grade 3 neutropenic infection plus grade 4 thrombocytopenia and S-1 dose interruption of ≥5 days. As defined in the protocol, the sunitinib dose was then increased to 37.5 mg/day on Schedule 2/2, where three of six patients experienced a DLT: grade 3 febrile neutropenia plus S-1 dose interruption of ≥5 days ($n=1$), grade 4 thrombocytopenia ($n=1$), and grade 4 neutropenia of ≥7 days ($n=1$).

All patients experienced at least one AE. No grade 5 AEs occurred. Serious AEs (SAEs) were reported in 13

Table 2 Baseline patient characteristics

	CDD schedule sunitinib 25 mg/day	Schedule 2/2 sunitinib 25 mg/day		Schedule 2/2 sunitinib 37.5 mg/day
	All patients (n=4)[a]	All patients (n=16)[b,c]	Patients with scirrhous-type disease (n=7)	All patients (n=6)[d]
Gender, male, n (%)	2 (50.0)	13 (81.3)	6 (85.7)	4 (66.7)
Age, years				
Median	63.0	60.0	57.0	60.5
Range	44–73	31–71	31–67	28–71
ECOG performance status, n (%)				
0	1 (25.0)	7 (43.8)	2 (28.6)	3 (50.0)
1	3 (75.0)	9 (56.3)	5 (71.4)	3 (50.0)
Measurable disease, n (%)	3 (75.0)	11 (68.8)	5 (71.4)	4 (66.7)
Histology, n (%)				
Diffuse	2 (50.0)	9 (56.2)	6 (85.7)	2 (33.3)
Intestinal	2 (50.0)	7 (43.8)	1 (14.3)	3 (50.0)
Other	0 (0)	0 (0)	0 (0)	1[e] (16.7)
Prior surgery, n (%)	1 (25.0)	5 (31.3)	1 (14.3)	2 (33.3)
Prior systemic therapy, n (%)				
0	2 (50.0)	16 (100.0)	7 (100.0)	5 (83.3)
1	2 (50.0)	0 (0)	0 (0)	1 (16.7)
≥2	0 (0)	0 (0)	0 (0)	0 (0)

CDD continuous daily dosing; *ECOG* Eastern Cooperative Oncology Group; *Schedule 2/2* 2 weeks on treatment followed by 2 weeks off treatment

[a] Includes one patient with scirrhous-type disease

[b] Includes 10 patients from the expansion cohort

[c] The subject assigned to sunitinib 25 mg/day on Schedule 2/2 who mistakenly received sunitinib 12.5 mg/day was excluded from the efficacy analyses. At baseline, this patient had an ECOG performance status of 0, stage IV measurable intestinal disease, with 2 involved tumor sites (liver and lymph node) and no prior surgery or systemic therapy

[d] No patients had scirrhous-type disease in this cohort

[e] This patient had mucinous histology

patients overall (48.1 %). Dose reductions due to AEs occurred for all three drugs: sunitinib: n=8; S-1: n=7; cisplatin: n=8. At the MTD, the median relative dose intensity (% actual/intended dose intensity) was 80.6 % (range, 32.4–100.0) for sunitinib (25 mg/day, Schedule 2/2), 68.2 % (35.7–85.7) for S-1, and 73.8 % (27.1–98.9) for cisplatin. Overall, seven patients discontinued the study treatment due to AEs, including four patients in the MTD cohort.

In the MTD cohort (sunitinib 25 mg/day, Schedule 2/2; n=16), the frequencies of common AEs of any grade are presented in Table 3. Neutropenia was the most frequently reported grade 3 or 4 AE, occurring in 15 patients (93.8 %). In total, 75.0 % of patients in the MTD cohort experienced grade 3 or 4 leukopenia. Fatigue, decreased appetite, nausea, constipation, thrombocytopenia, and stomatitis were the most common grade 1 or 2 AEs reported. In this cohort, SAEs occurred in eight patients (50.0 %); the most frequent SAEs were febrile neutropenia (n=3, 18.8 %) and platelet count decreased (n=2, 12.5 %).

Pharmacokinetics

The MTD combination of sunitinib (25 mg/day, Schedule 2/2) with S-1 plus cisplatin demonstrated no changes in the PK of sunitinib or its active metabolite (SU12662). In addition, combination treatment had no impact on the PK of cisplatin, tegafur, 5-FU, or S-1, compared with S-1 plus cisplatin alone (Table 4).

The mean trough plasma concentrations (C_{trough}) of sunitinib, SU12662, and total drug were 33.5 ng/mL, 13.9 ng/mL, and 47.5 ng/mL, respectively, for sunitinib 25 mg/day, and 69.9 ng/mL, 24.0 ng/mL, and 93.4 ng/mL, respectively, for sunitinib 37.5 mg/day. These C_{trough} values suggested that plasma concentrations of sunitinib increased in a dose-dependent manner.

Antitumor activity

All patients were evaluable for efficacy. In the MTD group (sunitinib 25 mg/day, Schedule 2/2), 11/16 patients had

Table 3 Treatment-emergent (all-causality) adverse events in ≥30 % of patients in the maximum tolerated dose cohort (sunitinib 25 mg/day on Schedule 2/2+cisplatin+S-1; n=16)

Adverse event, n (%)	Grade 1/2	Grade 3/4	All grades
Leukopenia	4 (25.0)	12 (75.0)	16 (100.0)
Neutropenia	1 (6.3)	15 (93.8)	16 (100.0)
Anemia	6 (37.5)	9 (56.3)	15 (93.8)
Decreased appetite	14 (87.5)	1 (6.3)	15 (93.8)
Thrombocytopenia	9 (56.3)	6 (37.5)	15 (93.8)
Fatigue	14 (87.5)	0	14 (87.5)
Nausea	14 (87.5)	0	14 (87.5)
Constipation	12 (75.0)	0	12 (75.0)
Stomatitis	9 (56.3)	0	9 (56.3)
Diarrhea	7 (43.8)	1 (6.3)	8 (50.0)
Dysgeusia	7 (43.8)	0	7 (43.8)
Pyrexia	7 (43.8)	0	7 (43.8)
Hiccups	6 (37.5)	0	6 (37.5)
Rash	5 (31.3)	0	5 (31.3)
Vomiting	5 (31.3)	0	5 (31.3)

Schedule 2/2 2 weeks on treatment followed by 2 weeks off treatment

measurable disease. No patients had a complete response, and partial responses occurred in 6/11 patients (54.5 %) with measurable disease, resulting in an overall objective response rate (ORR) of 37.5 % (95 % confidence interval [CI], 15.2–64.6) in 16 evaluable patients. A further six patients experienced no disease progression for ≥24 weeks, producing a CBR of 75.0 % (95 % CI, 47.6–92.7) among the 16 patients. Maximum percentage reduction in target lesion size in the 11 patients with measurable disease is shown in Fig. 2. The CBR for patients treated at the MTD with scirrhous-type disease was 57.1 % (95 % CI, 18.4–90.1; 4/7 patients). Tumor response in one patient with scirrhous-type disease is shown in Fig. 3. At the MTD, median PFS was 12.5 months (95 % CI, 6.4–16.5) and 6-month survival was 78.3 % (95 % CI, 56.5–100.0; Table 5; Fig. 4). Among the seven patients with scirrhous-type disease, four of five patients who had measurable lesion had a partial response, and median PFS was 12.5 months (95 % CI, 10.1–13.3).

Discussion

In this study, the MTD of sunitinib in combination with S-1 (80–120 mg) plus cisplatin 60 mg/m^2 was established as 25 mg/day on Schedule 2/2 in patients with advanced or metastatic gastric cancer for whom curative therapy was not an option. Other tested combinations included sunitinib 25 mg/day on a CDD schedule and a dose-increment from the MTD cohort to 37.5 mg; both cohorts were discontinued after DLTs were experienced. An additional 10 patients were then enrolled in the MTD cohort and followed for safety, antitumor activity, and PK parameters.

The MTD combination regimen demonstrated a manageable safety profile, with neutropenia and leukopenia as the most frequently reported grade 3 or 4 AEs: 93.8 % and 75.0 %, respectively. This safety profile was also consistent with a similar phase I dose-escalation study conducted in Western patients with advanced gastric cancer [23]. In general, the type of AEs was consistent with those previously reported when 5-FU and cisplatin were administered in patients with gastric cancer [24], although the frequency of events, particularly hematologic AEs, was greater than expected from previous studies of sunitinib in other tumor types [18, 25–28]. Previously reported mild skin reactions associated with sunitinib, such as yellowing skin/discoloration [29], were not observed in this study. There were no grade 3 or 4 non-

Table 4 Pharmacokinetics in the maximum tolerated dose cohort (sunitinib 25 mg/day on Schedule 2/2+cisplatin+S-1)

Treatment	Analyte	n	Mean C_{max} ng/mL (CV%)		Mean AUC_{last} ng·h/mL (CV%)	
			Sunitinib alone or SP	Combined	Sunitinib alone or SP	Combined
Sunitinib	Sunitinib	7	15.8 (32.2)	16.2 (44.6)	234 (25.3)	244 (38.6)
	SU12662	7	2.9 (43.6)	2.8 (49.3)	46.0 (34.2)	50.5 (50.7)
	Total drug	7	18.5 (33.0)	19.0 (42.3)	280 (25.0)	294 (37.2)
S-1	Tegafur	5	1,500 (9.8)	1,688 (26.9)	8,290 (10.5)	9,163 (12.7)
	5-FU	5	144 (23.5)	114 (16.5)	582 (19.3)	522 (28.0)
Cisplatin	Total	5	1,794 (7.8)	1,984 (3.6)	27,478 (7.1)	31,574 (5.4)
	Free	5	178 (68.3)	187 (74.6)	790 (25.8)	973 (28.3)

AUC_{last} area under the plasma concentration–time curve from time zero until last quantifiable observation; *C_{max}* maximum concentration; *CV* coefficient of variation; *5-FU* 5-fluorouracil; *Schedule 2/2* 2 weeks on treatment followed by 2 weeks off treatment; *SP* cisplatin 60 mg/m^2 every 28 days+S-1 40 mg/m^2 twice daily every 3/1 weeks; *SU12662* sunitinib active metabolite

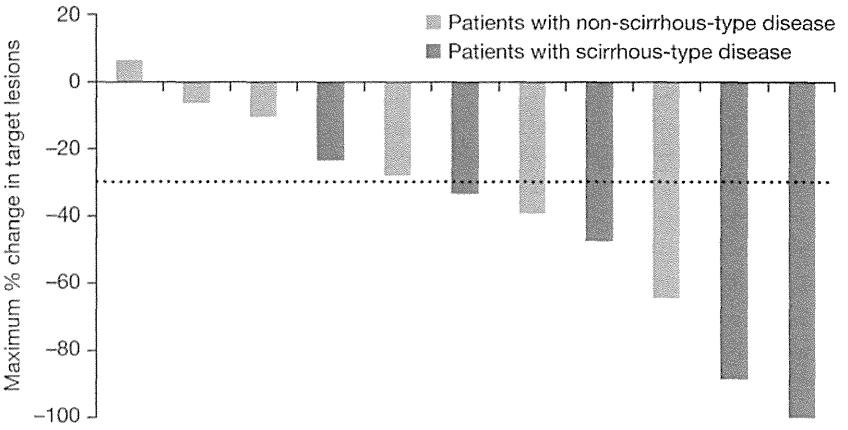

Fig. 2 Maximum percentage change in target lesion size in the maximum tolerated dose (MTD) cohort (sunitinib 25 mg/day on Schedule 2/2+cisplatin+S-1).[a] *Schedule 2/2* 2 weeks on treatment followed by 2 weeks off treatment. [a]Five of 16 patients receiving the MTD did not have measurable disease

hematologic events reported in ≥30 % of patients within the MTD cohort. No new safety signals were observed for sunitinib.

Although tumor evaluation was not the primary objective of this study, the ORR for the MTD cohort was 37.5 % (95 % CI, 15.2–64.6) and included responses in patients with scirrhous-type disease. Since five of 16 patients treated at the MTD did not have measurable disease and were assessed as non-responders in the ORR calculation, tumor response rates may be underestimated in our study. The ORR at the MTD among the 11 patients with measurable disease was 54.5 %. Median PFS was 12.5 months (95 % CI, 6.4–16.5) in the overall MTD cohort. These results demonstrate promising preliminary antitumor activity, compared with that observed for sunitinib as a single-agent modality in advanced gastric cancer, [18] and with the median PFS of 6 months reported for S-1 plus cisplatin [30]. However, our results must be interpreted with caution given the limited sample size studied.

A multitargeted tyrosine kinase inhibitor like sunitinib may be a promising drug for scirrhous gastric cancer. Our preliminary results suggest that sunitinib in combination

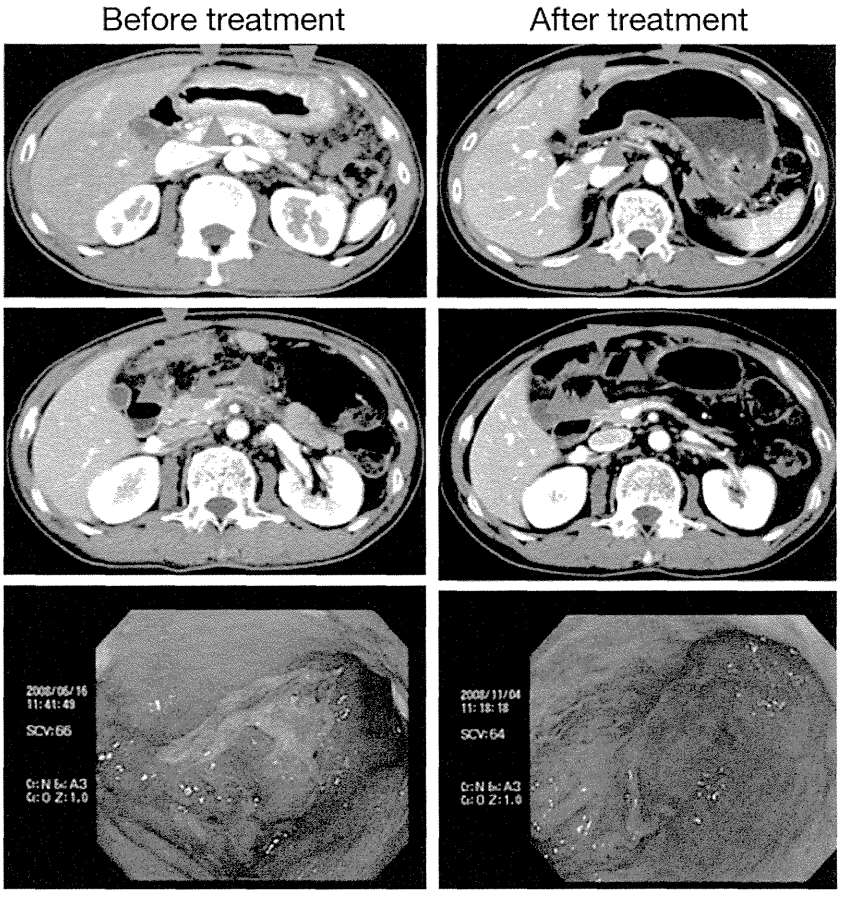

Fig. 3 Tumor response in a patient with scirrhous gastric cancer who received the maximum tolerated dose of sunitinib (25 mg/day on Schedule 2/2) combined with cisplatin and S-1. Blue arrowheads: primary lesion; orange arrowheads: peritoneal metastasis; green arrowheads: lymph node metastasis; *Schedule 2/2* 2 weeks on treatment followed by 2 weeks off treatment

Table 5 Summary of progression-free survival

	CDD schedule	Schedule 2/2	
	Sunitinib 25 mg/day (n=4)	Sunitinib 25 mg/day (n=16)[a]	Sunitinib 37.5 mg/day (n=6)
Patients with events, n (%)	2 (50.0)	9 (56.3)	4 (66.7)
Progression-free survival, months[b]			
Median	7.1	12.5	5.8
95 % CI	6.7–7.5	6.4–16.5	4.4–7.9
Probability of being event-free at month 6[c]			
Percentage	100.0	78.3	50.0
95 % CI[d]	100.0–100.0	56.5–100.0	1.0–99.0
Exploratory analysis: scirrhous-type disease			
		Schedule 2/2	
		Sunitinib 25 mg/day (n=7)[a]	
Patients with events, n (%)		4 (57.1)	
Progression-free survival, months[b]			
Median		12.5	
95 % CI		10.1–13.3	

CDD continuous daily dosing; *CI* confidence interval; *Schedule 2/2* 2 weeks on treatment followed by 2 weeks off treatment

[a] Maximum tolerated dose

[b] Based on the Brookmeyer and Crowley Method

[c] Estimated from the Kaplan–Meier curve

[d] Calculated from the product-limit method

with S-1 and cisplatin might have antitumor activity in patients with this disease type. However, as only seven of 16 patients at the MTD had scirrhous-type disease, caution should be used when interpreting these results. Despite this caveat, these data are encouraging, as scirrhous gastric cancer carries a worse prognosis than the non-scirrhous-type [31, 32], as it is characterized by rapid cancer cell infiltration and proliferation accompanied by extensive stromal fibrosis [32]. The proliferative and invasive ability of scirrhous gastric cancer cells have been shown to be closely associated with the growth factors produced by organ-specific fibroblasts and other stromal cells [32]. Therefore, targeting this cancer–stroma interaction using a multitargeted tyrosine kinase inhibitor such as sunitinib could be a reasonable treatment option for patients with scirrhous gastric cancer. However, large randomized studies would be required to confirm this hypothesis.

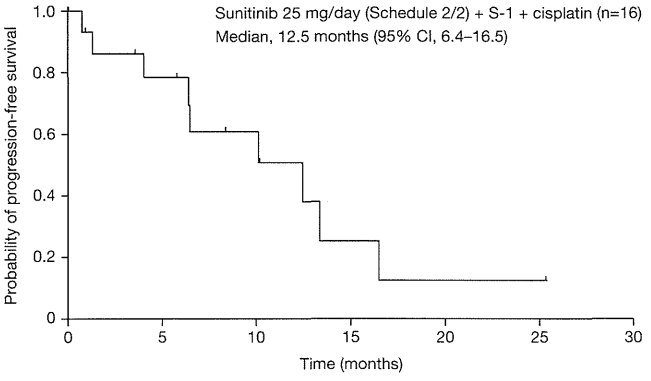

Fig. 4 Kaplan-Meier estimate of progression-free survival in the maximum tolerated dose cohort (sunitinib 25 mg/day on Schedule 2/2+ cisplatin+S-1). *CI* confidence interval; *Schedule 2/2* 2 weeks on treatment followed by 2 weeks off treatment

The combination of sunitinib with cisplatin plus S-1 demonstrated no PK drug–drug interactions, consistent with the different pathways of metabolism and elimination for these drugs. These findings are consistent with those from the phase I study with cisplatin plus 5-FU in Western patients [23]. The mean observed C_{trough} plasma concentration of 47.5 ng/mL, for total drug (sunitinib plus SU12662) at steady-state with sunitinib 25 mg/day dosing, in the present study suggests that optimal sunitinib exposure was almost achieved, in terms of the required concentration for target inhibition of ≥50 ng/mL [16].

In summary, the MTD of sunitinib was 25 mg/day on Schedule 2/2 in combination with cisplatin and S-1 when administered as a first-line therapy in patients with advanced or metastatic gastric cancer. This combination had a manageable safety profile and showed preliminary evidence of antitumor activity.

Acknowledgments We thank the participating patients and their families, as well as the investigators, research nurses, study coordinators, and operations staff. Medical writing support was provided by

Nicola Crofts and Molly Heitz (ACUMED®, Tytherington, UK) with funding from Pfizer Inc.

Conflict of interest Narikazu Boku, Nozomu Machida, Kei Muro, and Yoshinori Miyata have nothing to disclose.

Mariajose Lechuga and Nobuyuki Kimura are Pfizer Inc. employees and hold Pfizer Inc. stock.

Satoshi Hashigaki and Mie Suzuki are Pfizer Inc. employees.

Funding source This study was sponsored by Pfizer Inc.

Quantity of supporting information None

References

1. Jemal A, Bray F, Center MM, Ferlay J, Ward E, Forman D (2011) Global cancer statistics. CA Cancer J Clin 61:69–90
2. Inoue M, Tsugane S (2005) Epidemiology of gastric cancer in Japan. Postgrad Med J 81:419–424
3. Ajani JA (2007) Recent developments in cytotoxic therapy for advanced gastric or gastroesophageal carcinoma: the phase III trials. Gastrointest Cancer Res 1:S16–S21
4. Ajani JA, Barthel JS, Bekaii-Saab T, Bentrem DJ, D'Amico TA, Das P, Denlinger C, Fuchs CS, Gerdes H, Hayman JA, Hazard L, Hofstetter WL, Ilson DH, Keswani RN, Kleinberg LR, Korn M, Meredith K, Mulcahy MF, Orringer MB, Osarogiagbon RU, Posey JA, Sasson AR, Scott WJ, Shibata S, Strong VE, Washington MK, Willett C, Wood DE, Wright CD, Yang G (2010) Gastric cancer. J Natl Compr Canc Netw 8:378–409
5. Catalano V, Labianca R, Beretta GD, Gatta G, De BF, Van CE (2009) Gastric cancer. Crit Rev Oncol Hematol 71:127–164
6. Bang YJ, Van CE, Feyereislova A, Chung HC, Shen L, Sawaki A, Lordick F, Ohtsu A, Omuro Y, Satoh T, Aprile G, Kulikov E, Hill J, Lehle M, Ruschoff J, Kang YK (2010) Trastuzumab in combination with chemotherapy versus chemotherapy alone for treatment of HER2-positive advanced gastric or gastro-oesophageal junction cancer (ToGA): a phase 3, open-label, randomised controlled trial. Lancet 376:687–697
7. Glimelius B, Ekstrom K, Hoffman K, Graf W, Sjoden PO, Haglund U, Svensson C, Enander LK, Linne T, Sellstrom H, Heuman R (1997) Randomized comparison between chemotherapy plus best supportive care with best supportive care in advanced gastric cancer. Ann Oncol 8:163–168
8. Wagner AD, Grothe W, Haerting J, Kleber G, Grothey A, Fleig WE (2006) Chemotherapy in advanced gastric cancer: a systematic review and meta-analysis based on aggregate data. J Clin Oncol 24:2903–2909
9. Drescher D, Moehler M, Gockel I, Frerichs K, Muller A, Dunschede F, Borschitz T, Biesterfeld S, Holtmann M, Wehler T, Teufel A, Herzer K, Fischer T, Berger MR, Junginger T, Galle PR, Schimanski CC (2007) Coexpression of receptor-tyrosine-kinases in gastric adenocarcinoma–a rationale for a molecular targeting strategy? World J Gastroenterol 13:3605–3609
10. Zhang H, Wu J, Meng L, Shou CC (2002) Expression of vascular endothelial growth factor and its receptors KDR and Flt-1 in gastric cancer cells. World J Gastroenterol 8:994–998
11. Hassan S, Kinoshita Y, Kawanami C, Kishi K, Matsushima Y, Ohashi A, Funasaka Y, Okada A, Maekawa T, He-Yao W, Chiba T (1998) Expression of protooncogene c-kit and its ligand stem cell factor (SCF) in gastric carcinoma cell lines. Dig Dis Sci 43:8–14
12. Katano M, Nakamura M, Fujimoto K, Miyazaki K, Morisaki T (1998) Prognostic value of platelet-derived growth factor-A (PDGF-A) in gastric carcinoma. Ann Surg 227:365–371
13. Muller-Tidow C, Schwable J, Steffen B, Tidow N, Brandt B, Becker K, Schulze-Bahr E, Halfter H, Vogt U, Metzger R, Schneider PM, Buchner T, Brandts C, Berdel WE, Serve H (2004) High-throughput analysis of genome-wide receptor tyrosine kinase expression in human cancers identifies potential novel drug targets. Clin Cancer Res 10:1241–1249
14. Wagner AD, Moehler M (2009) Development of targeted therapies in advanced gastric cancer: promising exploratory steps in a new era. Curr Opin Oncol 21:381–385
15. Abrams TJ, Lee LB, Murray LJ, Pryer NK, Cherrington JM (2003) SU11248 inhibits KIT and platelet-derived growth factor receptor beta in preclinical models of human small cell lung cancer. Mol Cancer Ther 2:471–478
16. Mendel DB, Laird AD, Xin X, Louie SG, Christensen JG, Li G, Schreck RE, Abrams TJ, Ngai TJ, Lee LB, Murray LJ, Carver J, Chan E, Moss KG, Haznedar JO, Sukbuntherng J, Blake RA, Sun L, Tang C, Miller T, Shirazian S, McMahon G, Cherrington JM (2003) In vivo antitumor activity of SU11248, a novel tyrosine kinase inhibitor targeting vascular endothelial growth factor and platelet-derived growth factor receptors: determination of a pharmacokinetic/pharmacodynamic relationship. Clin Cancer Res 9:327–337
17. O'Farrell AM, Abrams TJ, Yuen HA, Ngai TJ, Louie SG, Yee KW, Wong LM, Hong W, Lee LB, Town A, Smolich BD, Manning WC, Murray LJ, Heinrich MC, Cherrington JM (2003) SU11248 is a novel FLT3 tyrosine kinase inhibitor with potent activity in vitro and in vivo. Blood 101:3597–3605
18. Bang YJ, Kang YK, Kang WK, Boku N, Chung HC, Chen JS, Doi T, Sun Y, Shen L, Qin S, Ng WT, Tursi JM, Lechuga MJ, Lu DR, Ruiz-Garcia A, Sobrero A (2010) Phase II study of sunitinib as second-line treatment for advanced gastric cancer. Invest New Drugs
19. Abrams TJ, Murray LJ, Pesenti E, Holway VW, Colombo T, Lee LB, Cherrington JM, Pryer NK (2003) Preclinical evaluation of the tyrosine kinase inhibitor SU11248 as a single agent and in combination with "standard of care" therapeutic agents for the treatment of breast cancer. Mol Cancer Ther 2:1011–1021
20. Yoon YK, Im SA, Min A, Kim HP, Hur HS, Lee KH, Han SW, Song SH, Youn OD, Kim TY, Kim WH, Bang YJ (2012) Sunitinib synergizes the antitumor effect of cisplatin via modulation of ERCC1 expression in models of gastric cancer. Cancer Lett 321:128–136
21. Lenz HJ, Lee FC, Haller DG, Singh D, Benson AB III, Strumberg D, Yanagihara R, Yao JC, Phan AT, Ajani JA (2007) Extended safety and efficacy data on S-1 plus cisplatin in patients with untreated, advanced gastric carcinoma in a multicenter phase II study. Cancer 109:33–40
22. Therasse P, Arbuck SG, Eisenhauer EA, Wanders J, Kaplan RS, Rubinstein L, Verweij J, Van Glabbeke M, van Oosterom AT, Christian MC, Gwyther SG (2000) New guidelines to evaluate the response to treatment in solid tumors. J Natl Cancer Inst 92:205–216
23. Gomez-Martin C, Gil-Martin M, Montagut C, Nunez JA, Salazar M, Puig R, Khosravan R, Tursi JM, Lechuga MJ, Bellmunt J (2010) A phase I, dose-finding study of sunitinib in combination with cisplatin and 5-fluorouracil in patients with advanced gastric cancer. Ann Oncol 21(Supplement 8):818P, abstr
24. Kang YK, Kang WK, Shin DB, Chen J, Xiong J, Wang J, Lichinitser M, Guan Z, Khasanov R, Zheng L, Philco-Salas M, Suarez T, Santamaria J, Forster G, McCloud PI (2009) Capecitabine/cisplatin versus 5-fluorouracil/cisplatin as first-line therapy in patients with advanced gastric cancer: a randomised phase III noninferiority trial. Ann Oncol 20:666–673

25. Burstein HJ, Elias AD, Rugo HS, Cobleigh MA, Wolff AC, Eisenberg PD, Lehman M, Adams BJ, Bello CL, DePrimo SE, Baum CM, Miller KD (2008) Phase II study of sunitinib malate, an oral multitargeted tyrosine kinase inhibitor, in patients with metastatic breast cancer previously treated with an anthracycline and a taxane. J Clin Oncol 26:1810–1816
26. Demetri DG, van Oosterom A, Garrett CR, Blackstein ME, Shah MH, Verweij J, McArthur G, Judson IR, Heinrich MC, Morgan JA, Desai J, Fletcher CD, George S, Bello CL, Huang X, Baum CM, Casali PG (2006) Efficacy and safety of sunitinib malate in patients with advanced gastrointestinal stromal tumor following failure of imatinib mesylate due to resistance or intolerance. N Engl J Med submitted
27. Motzer RJ, Hutson TE, Tomczak P, Michaelson MD, Bukowski RM, Rixe O, Oudard S, Negrier S, Szczylik C, Kim ST, Chen I, Bycott PW, Baum CM, Figlin RA (2007) Sunitinib versus interferon alfa in metastatic renal-cell carcinoma. N Engl J Med 356:115–124
28. Socinski MA, Novello S, Brahmer JR, Rosell R, Sanchez JM, Belani CP, Govindan R, Atkins JN, Gillenwater HH, Pallares C, Tye L, Selaru P, Chao RC, Scagliotti GV (2008) Multicenter, phase II trial of sunitinib in previously treated, advanced non-small-cell lung cancer. J Clin Oncol 26:650–656
29. Faivre S, Delbaldo C, Vera K, Robert C, Lozahic S, Lassau N, Bello C, DePrimo S, Brega N, Massimini G, Armand JP, Scigalla P, Raymond E (2006) Safety, pharmacokinetic, and antitumor activity of SU11248, a novel oral multitarget tyrosine kinase inhibitor, in patients with cancer. J Clin Oncol 24:25–35
30. Koizumi W, Narahara H, Hara T, Takagane A, Akiya T, Takagi M, Miyashita K, Nishizaki T, Kobayashi O, Takiyama W, Toh Y, Nagaie T, Takagi S, Yamamura Y, Yanaoka K, Orita H, Takeuchi M (2008) S-1 plus cisplatin versus S-1 alone for first-line treatment of advanced gastric cancer (SPIRITS trial): a phase III trial. Lancet Oncol 9:215–221
31. Yoshida M, Ohtsu A, Boku N, Miyata Y, Shirao K, Shimada Y, Hyodo I, Koizumi W, Kurihara M, Yoshida S, Yamamoto S (2004) Long-term survival and prognostic factors in patients with metastatic gastric cancers treated with chemotherapy in the Japan Clinical Oncology Group (JCOG) study. Jpn J Clin Oncol 34:654–659
32. Yashiro M, Hirakawa K (2010) Cancer-stromal interactions in scirrhous gastric carcinoma. Cancer Microenviron 3:127–135